

UNIVERSITÄTSKLINIKUM HAMBURG-EPPENDORF

Klinik und Poliklinik für Allgemein-, Viszeral- und Thoraxchirurgie

Direktor: Prof. Dr. med. Jakob R. Izbicki

Macrophage derived interleukin-10 promotes malignant pleural effusion formation

Dissertation

zur Erlangung des Grades eines Doktors der Medizin /Zahnmedizin
an der Medizinischen Fakultät der Universität Hamburg.

vorgelegt von:

Lilan Zhao

aus Fujian (China)

Hamburg 2019

(wird von der Medizinischen Fakultät ausgefüllt)

**Angenommen von der
Medizinischen Fakultät der Universität Hamburg am: 28.08.2019**

**Veröffentlicht mit Genehmigung der
Medizinischen Fakultät der Universität Hamburg.**

Prüfungsausschuss, der/die Vorsitzende: Prof. Dr. Nicola Gagliani

Prüfungsausschuss, zweite/r Gutachter/in: Prof. Dr. Eva Tolosa

CONTENTS

1. Introduction	5
1.1 Malignant Pleural Effusion (MPE)	5
1.1.1 The pathophysiology of MPE	6
1.2 Macrophage	9
1.2.1 The classification and functions of macrophages	10
1.2.2 Macrophage and MPE	12
1.3 T cell and MPE	12
1.4 IL-10 and cancer development	13
1.4.1 The discovery of IL-10	13
1.4.2 Stimulus of IL-10 expression	13
1.4.3 IL-10 receptor and its signal transduction	14
1.4.4 The target cells of IL-10	14
1.4.5 The influence of IL-10 on cancer	15
1.5 Aim of this study	16
2. Materials and Methods	17
2.1 Cancer cell lines	17
2.2 Animals	17
2.3 Cancer models	17
2.4 Human samples	18
2.5 Flow cytometry	18
2.6 Bioluminescence imaging	19
2.7 Enzyme-linked immunosorbent assays	19
2.8 Apoptosis Assay	20
2.9 Vascular Permeability Assays	20
2.10 Reverse transcriptase PCR, real-time qPCR	21
2.11 Single cell RNA sequencing	21
2.12 Single cell RNA-seq data analysis	22
2.13 Materials	23
2.14 Statistics	24
3. Result	25
3.1 Establishing the MPE model	25
3.2 Il-10 deficient mice are protected in MPE	25
3.3 Interleukin-10 mainly comes from myeloid cells	29

3.4	The transcriptional landscape of myeloid cells in the MPE	32
3.4.1	The functional state of the macrophages	43
3.5	The driving factor for the IL-10 secretion	45
3.6	The target cells of IL-10 in MPE	47
3.7	Dendritic cells derived Timp1 could promote MPE	49
3.8	Working hypothesis of IL-10 promoting MPE	54
4.	Discussion	55
5.	Summary/Zusammenfassung	62
6.	References	64
7.	Appendix	80
8.	Acknowledgement	82
9.	Curriculum Vitae	83
10.	Eidesstattliche Erklärung	84

1. Introduction

1.1 Malignant Pleural Effusion (MPE)

Pleural fluid is a thin layer of fluid which is present in the cavity formed by the visceral and parietal pleura. Under healthy conditions, the pleural fluid plays a key role as a lubricant for the respiratory movement.

There is a relatively constant dynamic balance between the production and absorption of the pleural fluid. However, when the pleura is subjected to pathological conditions, such as malignant tumor or infection, several factors lead to pleural effusion. These include increased pleural vascular permeability and occlusion of parietal pleural lymphatic vessels.

There are two types of pleural effusion: noninflammatory (transudative) effusion and inflammatory (exudative) effusion. The use of Light's criteria for differentiating transudative from exudative effusion, initially described in 1972, has been the standard method during the course of the past 45 years (**Table 1.1**) (Heffner et al., 1997; Light et al., 1972). Congestive heart failure and hepatic hydrothorax can cause benign pleural effusion which is the most common cause of transudative effusion. This is mainly due to hydrostatic pressure and decreased colloid osmotic pressure (Feller-Kopman and Light, 2018). While malignant pleural effusion (MPE), a common disease or complication in the clinic scenario, is classically exudative effusion, and the main cause is inflammation-increased vascular permeability. MPE is often the result of pleural metastasis in a variety of tumors, especially in advanced lung cancer (Light, 2013; Zamboni et al., 2015).

Table 1.1 Light's criteria for pleural effusions

	Transudate	Exudate
Protein (pleural/serum)	≤0.5	>0.5
LDH (pleural/serum)	≤0.6 Pleural LDH ≤ two-thirds upper limit of normal serum LDH	>0.6 Pleural LDH > two-thirds upper limit of normal serum LDH
Common causes	<ul style="list-style-type: none"> ·Hypoalbuminemia (cirrhosis, nephrotic syndrome) ·Congestive heart failure ·Constrictive pericarditis 	<ul style="list-style-type: none"> ·Infectious: bacterial, viral, tuberculosis-related, fungal, parasitic ·Neoplastic: metastatic disease (e.g., lung cancer, breast cancer), mesothelioma ·Pulmonary embolism ·Abdominal disease: pancreatitis, cholecystitis, hepatic or splenic abscess ·Autoimmune disease: rheumatoid arthritis, systemic lupus erythematosus, Sjögren's syndrome

(modified from Feller-Kopman, D. Light, R., Pleural Disease. 2018)

Two million patients die from MPE every year. In the U.S. alone, there are 200,000 cases per year (Clive et al., 2014; Zamboni et al., 2015). The prognosis is poor due to the lack of effective treatment. The median survival time is 4 to 6 months (Zamboni et al., 2015). Given the urgency and the short survival time, there is only a small temporal window available to gain and sustain therapeutic benefit (Murthy et al., 2019). Currently, patients with MPE are largely only provided with palliative care for symptomatic relief (Muduly et al., 2011). Therefore, there is an urgent need to identify therapeutic targets.

1.1.1 The pathophysiology of MPE

In general, MPE results from disrupted lymphatic drainage, increased capillary and pleura permeability, and increased fluid production (Psallidas et al., 2016).

Pleural fluid normally enters the pleural space through the systemic capillaries of both the parietal and the visceral pleura. Then, by absorptive pressure gradients through the parietal pleura and by cellular mechanisms, the volume of the fluid is

kept in balance by lymphatic drainage through the stomata of the parietal pleura (Feller-Kopman and Light, 2018).

According to the classical view, MPE is caused by tumor-associated blockade of local lymphatic drainage resulting in the impairment of effective pleural fluid absorption (Sahn, 1997). However, even though a lot of tumors cause lymphatic obstruction, not all of them induce MPE formation (Meyer, 1966; Sahn, 1997), indicating that blocking fluid removal from the pleural cavity cannot be the only cause of MPE formation.

Unlike the classical view, it has now been observed that there is increased vascular permeability leading to enhanced fluid production through excessive plasma leakage in MPE (Yano et al., 2000b). Both tumor cells and host cells can secrete several vasoactive mediators, which contribute to the development of MPE by increasing blood vessel leakiness, angiogenesis and inflammation. Such mediators include vascular endothelial growth factor (VEGF), interleukin (IL)-6, tumor necrosis factor (TNF), chemokine ligand 2 (CCL2) and secreted phosphoprotein-1 (SPP1, also known as osteopontin), angiopoietins and endostatin (Fang et al., 2009; Moschos et al., 2009; Nasreen et al., 2007; Yano et al., 2000b). For example, compared with benign pleural effusion, the levels of VEGF, IL-6 and angiogenin in MPE are significantly increased. In addition, VEGF levels are positively correlated with the volume of MPE, and immunotherapy targeting VEGF receptors reduced the MPE formation (Yano et al., 2000a; Yeh et al., 2006; Zebrowski et al., 1999). Bevacizumab and recombinant human endostatin are currently the two most commonly used anti-angiogenic drugs. Studies have shown that anti-angiogenic drugs could inhibit tumor-associated neovascularization (Ma et al., 2012; Peng et al., 2012). Osteopontin was reported to significantly promote the formation of MPE by promoting tumor cells and

mesothelial cells to secrete the VEGF to the extracellular matrix (Cui et al., 2015). Osteopontin also recruits macrophages into the pleural cavity and enhances the proinflammatory and angiogenic capacity of tumor cells. Finally, osteopontin can also directly stimulate blood vessels and increase the vascular permeability (Psallidas et al., 2013). These results indicated that the host-derived cytokine maybe amenable to therapeutic intervention.

Therefore, research on the pathophysiology of MPE has begun to shed light especially on the immune landscape of the malignant pleural space (**Figure 1.1**). Myeloid cells showed important roles in MPE formation. In human and mouse MPE, evidence suggests that mononuclear cells are probably the largest cellular population accrued to human and mouse MPE, and CCL2 is their major chemoattractant (Stathopoulos et al., 2008b). In addition, macrophages are a significant source of immunomodulatory signaling molecules important in MPE, including IL-6, transforming growth factor beta (TGF- β), CCL2, and Osteopontin (Psallidas et al., 2013; Stathopoulos et al., 2008b; Yeh et al., 2006). However, a functional role and the genetic landscape for the inflammatory myeloid cell populations in MPE remains to be determined. How did the immune cells infiltrate into the MPE environment? Are they infiltrating cells or expanded resident cells? How do the immune cells shape the high vascular permeability?

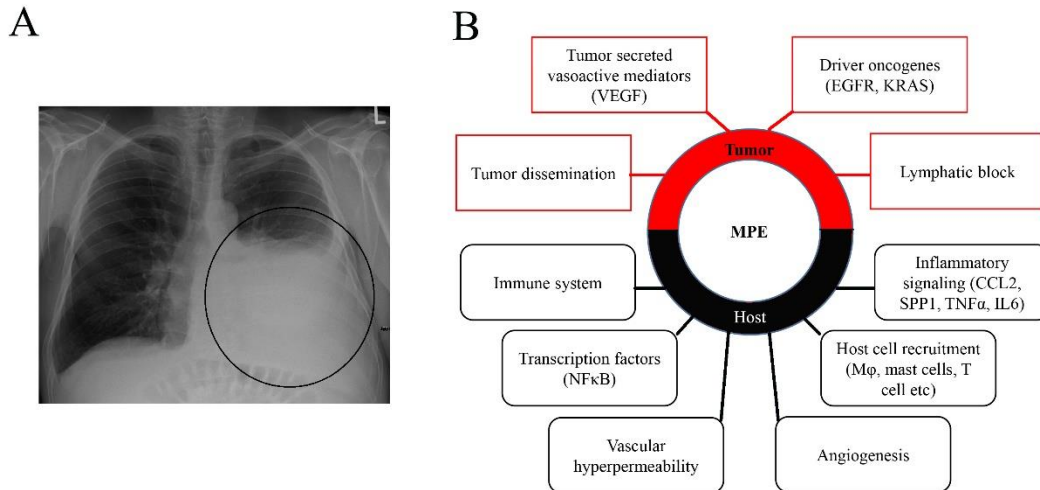


Figure 1.1.

A. The radiological manifestation of MPE. The left lower thoracic cavity is full of pleural effusion fluid. (modified from: Malignant Pleural Effusion, <https://www.newhealthadvisor.com/Malignant-Pleural-Effusion.html>)

B. MPE pathogenesis. Tumor-host interactions are key regulators of MPE formation. Tumor-elaborated vasoactive and inflammatory signaling, dictated by cancer cells, drives host-derived, MPE-related manifestations. The manifestations including angiogenesis, vascular hyperpermeability, and inflammation and host cell recruitment in the pleural microenvironment, ultimately resulting in MPE development. (modified from Spella et al., *J Thorac Dis.* 2015)

1.2. Macrophages

Increasing evidence indicates that immunoregulatory cells, such as tumor-associated macrophages, regulatory T cells (Tregs) and myeloid-derived suppressor cells (MDSCs), play an important role in promoting MPE formation (Li et al., 2016; Lv et al., 2014). Tumor associated macrophages, which are infiltrating in MPE, are a potential diagnostic and prognostic biomarker, and their frequency associates with the prognosis of MPE bearing lung cancer patients (Wang et al., 2015; Yang et al., 2015).

1.2.1 The classification and functions of macrophages

Macrophages are a heterogeneous cell population present in several tissues and they play a crucial role in regulating tissue homeostasis. However, they have also been implicated in various immune mediated pathologies (Jou et al., 2013). In human pleural effusions, macrophages represent more than half of all the cells (Kaczmarek and Sikora, 2012), but their role remains to be fully understood. Therefore, we decided to focus on this type of cell.

Under steady state conditions, the lung macrophages can be roughly classified into two categories according to their anatomical distribution: alveolar macrophages and interstitial macrophages. The former are distributed in the alveolar cavity, and their survival time is longer, with only 40% self-renewing rate in one year (Hashimoto et al., 2013); and the latter are mainly distributed in the alveolar interstitial, bronchial submucosa and adventitia, with a shorter survival period: a large number of cells are renewed every 21 days (Janssen et al., 2011).

In the tumor microenvironment, the infiltration and activation of macrophages, is an important marker of malignant tumors and plays a vital role in the interaction between the immune system and the tumor cells. Macrophages undergo different activations under different tumor microenvironmental stimuli, mainly including two types: (1) Classically activated macrophages, also known as M1 macrophages, with inhibition and killing of tumor cells; (2) Inducible activated macrophages, also known as M2 macrophages, mainly secrete anti-inflammatory cytokines such as arginase-1, IL-10 and transforming growth factor (TGF β), which can promote angiogenesis, and contribute to tumor growth and immunosuppression. Although still commonly used, and useful for conceptual understanding, the applicability of the M1/M2-classification is limited due to its oversimplification of the functional diversity of macrophages (Gordon and Martinez, 2010; Mosser and

Edwards, 2008). Considering the heterogeneity and plasticity of macrophages, new methods such as single cell RNA sequencing, which are able to provide an unsupervised characterization, are needed to accurately characterize the macrophage. This will help to better understand their function and relative contribution to tissue development, tissue remodeling and immune responses (Mosser and Edwards, 2008).

Macrophages could release a variety of cytokines, growth factors and chemokines. Therefore, they can participate in matrix remodeling by producing matrix metalloproteinases (MMPs) and cysteine cathepsins, also promoting tumor angiogenesis, lymphangiogenesis (for example, by vascular endothelial growth factor A (VEGFA), IL-8 and semaphorin 4D (SEMA4D)). Macrophages could exert immunosuppression and immune escape as well (for example, arginase 1 (ARG1), IL-10, programmed cell death 1 ligand 1 (PDL1) and TGF β), jointly promote tumor development, invasion and metastasis.

Notably, macrophages are able to phagocytose in order to clear pathogens, dead cells, and debris in order to regulate tissue homeostasis. Tyro3, Axl and Mertk, are members of the TAM (Tyro3-Axl-Mertk) subgroup of receptor tyrosine kinases (RTKs). Two closely related proteins— protein S (PROS1) and growth-arrest-specific 6 (GAS6)— serve as cognate ligands that bind and activate the TAM receptors (Stitt et al., 1995). Apoptotic tumor cells expose phosphatidylserine (PtdSer) on their surfaces as an “eat-me” signal. Hence, GAS6 and PROS1 ligands function as bridges between a PtdSer-exposing cell and a TAM receptor-bearing cell, therefore activating the TAM RTKs on the surface of phagocytes, such as macrophages. Efferocytosis by macrophages can lead to the expression of factors such as ARG1, TGF- β , and IL-10.

1.2.2 Macrophage and MPE

Macrophages constitute over half of all the cells found in the pleural space (Murthy et al., 2019). Decreased CD163⁺ (one of the M2 markers, a scavenger receptor for haptoglobin–hemoglobin complexes that is mostly expressed by monocytes and macrophages) macrophages could predict NSCLC MPE progression free survival (PFS) (Yang et al., 2015). In MPE, macrophages promote angiogenesis by releasing proangiogenic chemokines (CXCL1, CXCL2, CXCL8), cytokines (TNF- α , IL-1 α , IL-1 β , IL-6), and growth factors (TGF- α , VEGF, PDGF, angiopoietins), thus promoting micro-vessel formation, vascular leakiness and subsequent MPE development (Ellis et al., 2001). Macrophages can also impact other cells in the setting of MPE. They can for example, modulate T cell proliferation and differentiation by releasing IL-1 β , TNF- α , and IL-8 (Kaczmarek and Sikora, 2012; Park et al., 2003).

1.3 T cell and MPE

The CD4⁺ T helper cells (Th cells) are the primary orchestrators of the adaptive immune response, mediating a variety of cellular and humoral responses against pathogens and cancer (Sun and Zhang, 2014). Th cells can be subdivided into different subsets based on a master transcriptional regulator and a unique cytokine profile: for example, Th17 cells express ROR γ t that in turn promotes the transcription of *Il17a*, *Il17f*, *Il21* and *Il22*. Th1 cells express T-bet and produce IFN- γ , IL-2 and TNF- α . Th2 cells express GATA-3 and secrete IL-4, IL-5 and IL-13 (Zhu et al., 2010). It is well known that Th cells dominance occurs in MPE (Lucivero et al., 1988). Previous data demonstrated that the interaction between tumor cells and multiple subgroups of Th cells (such as Th9, Th17 and Th22) (Ye et al., 2010; Ye et al., 2012a; Ye et al., 2012b), and regulatory T cells (Chen et al., 2005), contributes to the pathogenesis of MPE. For example, while Th1 differentiation was traditionally thought to promote antitumor responses, IFN- γ

deficient mice, devoid of Th1 and rich in Th17 cells, were protected from MPE development, while IL-17A deficient mice, rich in Th1 and devoid of Th17 cells, had enhanced pleural tumor cell proliferation and vascular leakiness (Lin et al., 2014).

1.4. IL-10 and cancer development

1.4.1 The discovery of IL-10

Cytokines are major regulators of both innate and adaptive immunity. They allow cells of the immune systems to communicate over distance in paracrine and autocrine fashion (Arango Duque and Descoteaux, 2014). They control proliferation, differentiation, effector functions, and survival of leukocytes (Waldmann, 2018). Among cytokines, interleukin-10 (IL-10) is a prototypical anti-inflammatory cytokine. In 1989, Mosmann *et al.* (Fiorentino et al., 1989) discovered the cytokine synthesis inhibitory factor (CSIF), which was found to be part of the interleukin family and therefore was also named IL-10. In addition to T cells, many immune cells have the ability to produce IL-10, including macrophages, B cells, mast cells, eosinophils, and dendritic cells. Finally, it has been recently reported that IL-10 could promote MPE formation (Wu et al., 2019).

1.4.2 Stimulus for IL-10 expression

IL-10 production in myeloid cells is largely triggered by various signals downstream of various pattern recognition receptors (PRRs), like Toll-like receptors (TLRs). Co-stimulatory receptor pathways such as CD40, Dectin-1, and CD209 can synergize with TLR pathways to regulate IL-10 production (Gabrysova et al., 2014). Also, proinflammatory cytokines like type I IFN can also modulate the expression of IL-10 in myeloid cells (Ouyang and O'Garra, 2019). In addition, when macrophages ingest apoptotic cells through TAM receptors, they upregulate the production of immunosuppression cytokines, such as IL-10 (Akalu

et al., 2017; Voll et al., 1997). For example, Cook *et al.* showed lower amounts of IL-10 in tumor-derived *Mertk*^{-/-} CD11b⁺ cells than in *Mertk*^{+/+} CD11b⁺ cells (Cook et al., 2013). At the transcription level, Chung *et al.* (Chung et al., 2007) showed IL-10 production stimulated by apoptotic cells was regulated by p38 mitogen-activated protein kinase (MAPK) and required cell-cell contact. They showed that apoptotic cell response element (ACRE) mediates the transcriptional activation of IL-10 via both pre-B-cell leukemia transcription factor-1b (Pbx-1b) and Hox cofactor Pbx-regulating protein 1 (Prep-1).

1.4.3 IL-10 receptor and its signal transduction

IL-10R belongs to the class II cytokine receptor family and consists of two distinct chains, IL10R α (also referred to as IL10R1) molecule (encoded by the *Il10ra* gene) and IL10R β (also referred to as IL10R2) molecule (encoded by the *Il10rb* gene) (Kotenko et al., 1997; Moore et al., 2001). The binding of IL-10 to the IL-10R takes place in two steps: First, IL-10 binds IL-10R1 with high specificity, and the interaction of IL-10/IL-10R1 changes the spatial structure of IL-10. Then this complex will be combined with IL-10R2 (Moore et al., 2001). Without the help of IL-10R2, IL-10 does not function even in combination with IL-10R1, so the functions of both are equally important and indispensable (Redford et al., 2011). The engagement of the IL-10 with the IL-10 receptor promotes the phosphorylation of the JAK1 and TYK2 pathways, thereby activating STAT3 (signal transducers and activators of transcription 3) (Sabat et al., 2010), which is the indispensable Stat molecule mediating the downstream transcription of target genes induced by IL-10.

1.4.4 The target cells of IL-10

IL10R α is expressed on hematopoietic cells under physiological conditions. However, it can be up regulated upon activation, which suggests the importance

of this receptor in controlling overwhelming immune responses (Shouval et al., 2014). For example, IL10R α expression is low in naïve CD4⁺ T cells under steady state, but after *in vivo* anti-CD3 treatment, IL10R α expression increased on Th17 cells in the small intestine (Huber et al., 2011). Also, *in vitro* stimulation of naïve CD45RB^{high} T cells, memory/effector T cells, and Foxp3⁺ Treg cells leads to upregulation of IL10R α expression (Kamanaka et al., 2011). IL10R α is also on innate cells of the innate immune system. Under basal conditions, neutrophils express low levels of IL10R α . However, IL10R α expression is upregulated following lipopolysaccharide (LPS) or IL-4 stimulation (Crepaldi et al., 2001). Furthermore, IL10R α can also be expressed by non-immune cell types such as epithelial cells (Bourreille et al., 1999; Denning et al., 2000), keratinocytes and fibroblasts (Weber-Nordt et al., 1994), usually upon induction rather than constitutively. In contrast, IL10-R β is ubiquitous in most cells and tissues under steady state conditions (Gibbs and Pennica, 1997; Lutfalla et al., 1993).

1.4.5 The influence of IL-10 on cancer

There are studies showing that both human and mouse lung cancer cells could induce T cells to produce IL-10, which could promote lung cancer growth by suppressing both T cell and APC antitumorigenic functions. For example, IL-10 block cytotoxic T lymphocytes (CTL) responses and IL-12 production (Huang et al., 1996; Sharma et al., 1999). Zeni *et al.* (Zeni et al., 2007) found a poor prognosis in patients with high expression of IL-10 in tumor-associated macrophages in non-small cell lung cancer tissues. At present, IL-10 can directly inhibit the proliferation and migration of effector T cells and down-regulate the production of related cytokines, playing an important role in inducing immune escape of tumors. When IL-10 levels are increased, the cytotoxic effect of T cells on tumor cells is significantly inhibited. Blocking IL-10 in animal models can

increase the killing ability of the immune system to tumor cells (Mocellin et al., 2004; Tanikawa et al., 2012). In addition, studies have shown that IL-10 can also form an immunosuppressive environment by inhibiting the activation of APC, thereby inducing tumor immune escape (Mittal and Roche, 2015). In contrast to these findings, Kohno *et al.* demonstrated that IL-10 could inhibit the growth and peritoneal dissemination of the tumor *via* the inhibition of vascular endothelial growth factor (VEGF)-mediated angiogenesis, resulting in improved survival (Kohno et al., 2003). IL-10 concentration was found elevated in MPE (Chen et al., 1996; Klimatsidas et al., 2012), and IL-10 can promote MPE in mice by regulating Th1- and Th17-cell differentiation and migration (Wu et al., 2019). However, the function, the source and the target cells of IL-10 in MPE remain unclear.

1.5. Aim of this study

Tumor cells orchestrate a complex immune network, composed of host cells (i.e. pleural macrophages, pleural mesothelial cells, etc.) and recruited cells (i.e. monocytes, mast cells, neutrophils and lymphocytes etc.). The interactions between the tumor cells and the immune cells lead to a sharp increase in the levels of inflammatory factors and vasoactive factors in the pleural space, thereby increasing pleural vascular permeability and leading to the production of pleural effusion. Therefore, MPE is considered to be an immune and vascular-mediated clinical manifestation of tumor metastasis to the pleura. The causes of MPE are complex and here the aim is to further examine the microenvironment of MPE, especially the accurate characterization of the relationship between MPE and macrophages in order to enable the development of innovative diagnostic and therapeutic strategies.

2. Materials and Methods

2.1 Cancer cell lines

LLC (NCI Tumor Repository, Frederick, MD) and MC38 cells (Marazioti et al., 2013) were cultured at 37 °C in 5% CO₂-95% air using DMEM supplemented with 10% FBS, 1 mM pyruvate, 2 mM L-glutamine, 100 mg/ml streptomycin, and 100 U/ml penicillin. For in vivo injections, cells were harvested and counted as described elsewhere, and injected through a left intercostal space, as described elsewhere (Marazioti et al., 2013; Stathopoulos et al., 2007; Stathopoulos et al., 2008a; Stathopoulos et al., 2010; Stathopoulos et al., 2006).

2.2 Animals

C57BL/6 mice were obtained from The Jackson Laboratory (Bar Harbor, MN), IL-10^{Th1.1} (CD90.1) mice were kindly provided from C. Weaver (Maynard et al., 2007), IL10^{-/-} mice (Kuhn et al., 1993), Foxp3^{mRFP} (Wan and Flavell, 2005) and IL-10^{eGFP} (Kamanaka et al., 2006) reporter mice are described elsewhere. Age and sex-matched littermates between 8 and 16 weeks of age were used. All mice were in a C57BL/6 background. Animals were maintained under specific pathogen-free conditions and handled according to protocols approved by the responsible federal health Authorities of the State of Hamburg (Behörde für Gesundheit und Verbraucherschutz). All animal experiments were performed in accordance with national and institutional guidelines and regulations.

2.3 Cancer models

In order to achieve MPE formation, 150,000 murine cancer cells were administered intrapleurally to mice which were then killed 14 days post injection. Intrapleural injections were performed under direct stereoscopic vision through an incision in the left anterolateral chest skin and fascia. For this, a 27 G needle

was inserted in the pleural cavity at a 45° angle under direct contact with the superior rib and the tumor cell suspensions were injected under direct visual inspection (**Figure 2.1**). For pleural lavage, 1 mL normal saline was injected intrapleurally and was withdrawn starting after 30 seconds waiting time.



Figure 2.1. For induction of malignant pleural effusion, after anesthesia with isoflurane, mice underwent a left lateral thoracic incision (**A**), 100µl PBS containing 150,000 cancer cells was intrapleurally injected (**B**) and the incision were closed by metal clamps (**C**).

2.4 Human samples

Pleural fluid samples were received during diagnostic thoracenteses in patients suffering from MPE caused by lung cancer (n = 18), other cancers (n = 11), as well as patients with parapneumonic pleural effusion (PPE) (n =16) and transudative pleural effusion (TrPE) (n =17) treated at the Department of Respiratory Medicine, University of Thessaly, BIOPOLIS, Larissa, Greece. All protocols abided by the Helsinki Declaration, were approved a priori by the local hospital ethics committees and by all patients via written informed consent.

2.5 Flow cytometry

The cell suspension was filtered through 100 µm and 40 µm cell strainers and centrifuged at 400 x g, 5 min at 4 °C. Cells were resuspended in cell blood lysis buffer (0.15 M NH₄Cl, 10 mM KHCO₃, 0.1 mM EDTA) for 5 min, washed in PBS and re-suspended in FACS-buffer (PBS, 2 mM EDTA, 25 mM HEPES) at 1 million cells/100 µl and incubated for 20 min on ice with a mixture of appropriate

antibodies (**Table 2.1**) (1 μ l/5 million cells). Labeled cells were washed with PBS and resuspended in FACS-buffer. Cells were labelled with eBioscience™ Fixable Viability Dye eFluor™ 506 (cat# 65-0866-14) for cell viability.

For intracellular cytokine staining the cells were re-stimulated for 3 h at 37 °C with phorbol 12-myristate 13-acetate (PMA) (Sigma, 50 ng ml⁻¹) and ionomycin (Sigma, 1 mg ml⁻¹) in the presence of Golgistop (BD Bioscience). Cells were then fixed in paraformaldehyde for 20 min at room temperature. After washing, the cells have been permeabilized (NP40) and stained at 4 °C with intracellular antibodies for 30 min. The flow cytometric analyses were performed with BD LSRFortessa™ cytometer (BD Biosciences, Alameda, CA), and data were examined using FlowJo software (FlowJo, Ashland, OR). Additionally, data were analyzed using the Cytobank platform (viSNE analysis).

2.6 Bioluminescence imaging

Cells and mice were serially imaged on a Xenogen Lumina II and, after addition of 300 μ g/mL D-luciferin to culture media or i.v. delivery of 1 mg D-luciferin. Data were analyzed using Living Image v.4.2 (Perkin-Elmer, Waltham, MA). (Marazioti et al., 2013; Stathopoulos et al., 2007; Stathopoulos et al., 2010; Stathopoulos et al., 2006)

2.7 Enzyme-linked immunosorbent assays

IL-10 level of cell culture supernatants, of cell-free MPE, and sera were determined using dedicated murine ELISA kits according to the manufacturer's instructions (Peprotech, London, UK and R&D, Minneapolis, MN).

An indicated protocol for ELISA:

Recommended buffers:

PBS 1X, wash buffer (0.05% Tween-20 in PBS), block buffer (1% BSA in PBS), diluents buffer (0.05% Tween-20, 0.1% BSA in PBS)

Procedure:

First of all, the 96-well plate was coated by capture antibody and was incubated overnight at room temperature. On the next day, the plate was washed 4 times using 300µl of wash buffer per well. Then, it was blocked for at least 1 hour at room temperature. 100µl of standard or sample was loaded to each well in triplicate. Samples were incubated at room temperature for at least 2 hours. After washing, detection antibody was added in each well and the plate was incubated. After 2 hours, the wells were aspirated and the plate was washed. Avidin-HRP conjugate was added in each well. After 30 minutes, the liquid was aspirated and the substrate solution was added in each well. The plate was incubated at room temperature for color development. Color development was monitored by an ELISA plate reader at 405 nm with wavelength correction set at 650 nm.

2.8 Apoptosis Assay

Apoptotic cells were examined using Annexin V-FITC Apoptosis Detection Kit (ab14085 Abcam, Cambridge, UK) following the manufacturer's instructions. Briefly, cells were harvested by careful centrifugation, washed twice with 1* Annexin V binding buffer, resuspended in binding buffer, and stained with Annexin V and PI. Cell apoptosis was detected using the FACS (BD LSRFortessa™, BD Biosciences).

2.9 Vascular Permeability Assays

Mice with MPE received *i.v.* 0.8 mg Evans' blue and were killed after one hour and the albumin-binding dye levels in the MPE were determined (Stathopoulos et al., 2007). Intradermal injections of PBS (1.5 ng/50 µL), cell-free MPE (50 µL), or cancer cell-conditioned media (50 µL) performed at different spots of the shaved

dorsal mouse skin were followed by immediate Evans' blue injections as above. One hour post injection the mice were killed, their skin was inverted and imaging of the skin was performed. The surface area of dye leak was determined using Fiji academic freeware (<http://fiji.sc/Fiji>), as described elsewhere (Marazioti et al., 2013; Stathopoulos et al., 2008a; Stathopoulos et al., 2010).

2.10 Reverse transcriptase PCR, real-time qPCR

RNA isolation was performed using TRIzol LS reagent (Life Technology) according to the manual. The isolated RNA was subjected to reverse transcription with High-Capacity cDNA Reverse Transcription Kit (Thermo Fisher Scientific). cDNA was semi quantified using commercially available primer/probe sets from Applied Biosystems or using SYBR Green Master Mix in a StepOnePlus cycler (Applied Biosystems, Carlsbad, CA). Samples were analyzed with the change in cycle threshold method. Results were normalized to hypoxanthine phosphoribosyltransferase (*Hprt*), quantified in parallel amplification reactions. Reverse transcriptase-PCR primers are given in **Table**

2.2.

2.11 Single cell RNA sequencing

Single-cells were encapsulated in droplets using 10X Genomics GemCode Technology and processed following manufacturer's specifications. Briefly, every cell and every transcript are uniquely barcoded using a unique molecular identifier (UMI) and cDNA ready for sequencing on Illumina platforms is generated using the Single Cell 3' Reagent Kits v2 (10X Genomics). Libraries were sequenced across a HiSeq 4000 (Illumina) in paired-end to reach approximately 50,000 reads per single-cell.

2.12 Single cell RNA-seq data analysis

Data was demultiplexed using CellRanger software (version 2.0.2) based on 8 base pair 10X sample indexes and paired-end FASTQ files were generated. The cell barcodes and transcript UMIs were processed as previously described (Zheng et al., 2017). The reads were aligned to mouse UCSC mm10 reference genome using STAR aligner. The alignment results were used to quantify the expression level of mouse genes and generation of gene-barcode matrix. “cellranger aggr” command of CellRanger was used for aggregating different libraries from multiple sequencing runs. Low quality cells, doublets and potentially dead cells were removed according the percentage of mitochondrial genes and number of genes and UMIs expressed in each cell. The remaining data was normalized and log transformed and the log transformed matrix was used for all downstream analysis. Data clustering was performed using Seurat R package (Satija et al., 2015). Highly variable genes - genes with relatively high average expression and variability - were detected with Seurat and these genes were used for downstream clustering analysis. Principle component analysis (PCA) was used for dimensionality reduction and the number of significant principle components was calculated using built in “JackStraw” function. t-distributed stochastic neighbor embedding (t-SNE) was used for data visualization in two dimensions. Two complementary approaches were used to identify differentially expressed genes. In results of Seurat package, genes with p values smaller than 0.01 were considered as differentially expressed genes.

Preprocessing Analysis with Seurat Package

The Seurat pipeline was applied to the dataset. Genes that were expressed in less than 3 cells and cells that expressed less than 200 and more than 4000 genes, were excluded. Data was normalized with a scale factor of 10^4 . Latent variable- number of UMI's - were regressed out using a negative binomial model

(function ScaleData). Most variable genes were detected by the FindVariableGenes function and used for subsequent analysis. Principle component analysis (PCA) was performed on about 2,000 genes with PCA function. A tSNE dimensional reduction was performed on the scaled matrix (with most variable genes only) using first 15 PCA components to obtain a two-dimensional representation of the cell states. For clustering, we used the function FindClusters that implements SNN (shared nearest neighbor) modularity optimization based clustering algorithm on 15 PCA components with resolution 0.6, leading to 8 clusters for the analysis.

Identification of Cluster-Specific Genes and Marker-Based Classification

To identify marker genes, the FindAllMarkers function was used with likelihood-ratio test for single cell gene expression. For each cluster, only genes that were expressed in more than 25% of cells with at least 0.25-fold difference were considered. To perform gene ontology analysis, we used clusterProfiler (3.12.0). For heatmap representation, mean expression of markers inside each cluster was used.

2.13. Materials

Table 2.1. Flow Cytometry Antibodies

Target	Provider	Catalog #	Dilution	Conjugate
CD45 (30-F11)	Biologend	103149	1:800	BV785
CD3 (17A2)	BD Biosciences	740268	1:400	BUV395
CD4 (GK1.5)	Biologend	5100736	1:600	AF700
CD8a (53-6.7)	Biologend	100714	1:400	APC/Cy7
CD11b (M1/70)	Biologend	101216	1:400	Pe/Cy7
F4/80 (BM8)	BD Biosciences	53-4801-82	1:400	AF488
Ly6c (HK1.4)	Biologend	128030	1:400	BV570
Ly6g (1A8)	Biologend	204927	1:400	AF647
CD90.1 (Thy1.1)(OX-7)	Biologend	202526	1:400	APC
CD210(IL10R) (1B1.3a)	Biologend	112706	1:100	PE
pStat3 (pY705)	BD Biosciences	560312	1:5	Pacific Blue
IL-10 (JES5-16E3)	Biologend	210714	1:100	AF647
Fixable Viability Dye eFluor™ 506	eBioscience	65-0866-14	1:1000	Amcyan

Table 2.2. Related to Experimental Procedures.

PCR primers used for this study			
Method	Primer	Sequence/ TaqMan Gene Expression Assays IDs	Length
qPCR			
	Il10	Mm01288386_m1	136 bp
	Timp1	Mm01341361_m1	100 bp
	Il10ra	Mm00434147_m1	66 bp
	Il10rb	Mm00434157_m1	69 bp
genotyping			
	IL-10fw	GCC TTC AGT ATA AAA GGG GGA CC	200 bp/
	IL-10rev	GTG GGT GCA GTT ATT GTC TTC CCG	450 bp
	IL10 neo	CCT GCG TGC AAT CCA TCT TG	
	TIGER IL-10 F	GTG TGT ATT GAG TCT GCT GGA C	350 bp
	TIGER IL-10 R1	GTG TGG CCA GCC TTA GAA TAG	
	TIGER IL-10 R2	GGT TGC CTT GAC CAT CGA TG	
	TIGER GFP-5'	GGA CGT GGT TTT CCT TTG AA	200 bp
	TIGER GFP-3	GAA CTT CAG GGT CAG CTT GC	
	BIT-1	GTT CAT TCC GAC CAG TTC TTT AGC	1250 bp
	BIT-2	TCC TTG GGG TCT TCT ACC TTT CTC	

2.14 Statistics

Sample size was calculated using power analysis on G*power academic freeware (Faul et al., 2007), assuming $\alpha = 0.05$, $\beta = 0.8$, and $\rho = 0.3$ (<http://www.gpower.hhu.de/>). Animals were distributed to different treatment groups by alternation and transgenic animals were enrolled case-control-wise. Data were collected by at least two blinded investigators from samples coded by a non-blinded investigator. All data were examined for normality of distribution by Kolmogorov-Smirnov test. Normally and not normally distributed values are given as mean \pm SEM and median \pm interquartile range, respectively. Sample size (n) always refers to biological and not technical replicates. Differences in means between two or multiple groups were examined, respectively by t-test or one-way ANOVA with Bonferroni post-hoc tests, and in medians between two or multiple groups by Mann-Whitney U-test or Kruskal-Wallis test with Dunn's post-hoc tests, as appropriate. Correlations were done using Pearson's R or Spearman's ρ , as appropriate. All p values are two-tailed and were considered significant when $<.05$. All statistical analyses were done and plots were created using Prism v8.0 (GraphPad, La Jolla, CA).

3. Result

3.1. Establishing the MPE model.

To validate our MPE mouse model, we injected the MPE-competent Lewis lung carcinoma cancer cell line (LLC) into C57BL/6 mice. In particular, we injected 1.5×10^5 mouse cancer cells into the pleural cavities of the mice (**Figure 3.1 A**). Upon pleural injection, LLC cell line produced extensive pleural carcinomatosis which ultimately lead to MPE (**Figure 3.1 B**).

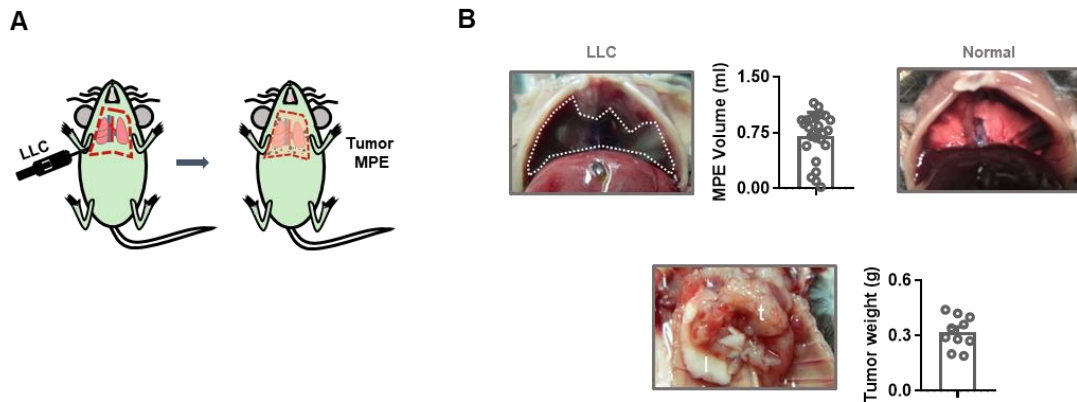


Figure 3.1. Validation of the MPE model.

(A). Scheme of the malignant pleural effusion (MPE) model. MPE was induced via intrapleural injection of mice with cancer cell.

(B). (Upper panel) Representative images of MPEs (dashed lines), data summary of MPE volume and representative images of a normal thoracic cavity. (Lower panel) Representative images of pleural tumors (t) and lungs (l) and data summary of pleural tumor mass.

3.2. Il-10 deficient mice are protected in MPE.

IL-10 is an important immunosuppressive cytokine which is frequently elevated in tumor microenvironment. It has been suggested that IL-10 promote MPE in mice by regulating Th1- and Th17-cell differentiation and migration (Wu et al., 2019). Since IL-10 deficient mice have different degrees of enterocolitis in different animal facilities and since intestinal inflammation could be a confounding factor,

we wondered whether we could reproduce a similar phenotype in our facility. We used IL-10 deficient mice, which were kept under specific-pathogen-free (SPF) conditions and did not show enterocolitis (data not shown) (Kuhn et al., 1993). Depletion of IL-10 abrogated MPE formation induced by LLC cancer cell line (**Figure 3.2 B**). We further confirmed this result using a different tumour cell line: MC38 colorectal adenocarcinoma cell line (**Figure 3.2 E**). However, using both cell lines we observed not obvious effect on tumor growth comparing the wild type with the IL-10 deficient mice (**Figure 3.2 C**; **Figure 3.2 D**; **Figure 3.2 F**). From this point on we decided to use only the LLC cell line. We observed that the survival was longer in IL-10 deficient mice compared to wildtype littermate control (**Figure 3.2 G**) under LLC induced MPE conditions, which suggested that poor survival was mainly due to the MPE formation.

Pleural vascular leakiness is a prerequisite of pleural fluid production and a key element of MPE pathobiology (Psallidas et al., 2016). To explore whether IL-10 influences this parameter, we determined pleural fluid levels of albumin-binding Evans' blue dye, which had been intravenously injected 1 h before sacrificing. Pleural vascular permeability was markedly reduced in the absence of IL-10 (**Figure 3.2 H**), suggesting that IL-10 is a pro-permeability factor.

Taken together, these results suggested that IL-10 in MPE is associated with induction of an inflammatory, angiogenic, and vasoactive response in the pleural space, but not with enhanced tumor growth.

Then, on the basis of expression of the following surface markers: CD45, CD3, CD11b (**Table 2.1**), we used one dimension-reduction algorithm referred to as visualization of t-distributed stochastic neighbor embedding (viSNE) to visualize to cellular composition in MPE (Amir el et al., 2013). Using viSNE we gated on CD45⁺ singlets and analyzed 100,000 events per sample. In the viSNE plots, each dot represents a single cell positioned in a multidimensional space. Compared with IL-10^{-/-} mice, the frequencies of CD3⁺ and CD11b⁺ cells are

similar in the MPE and pleural tumors of the littermate wildtype mice which is showed by column plot and viSNE plot (**Figure 3.2 I**).

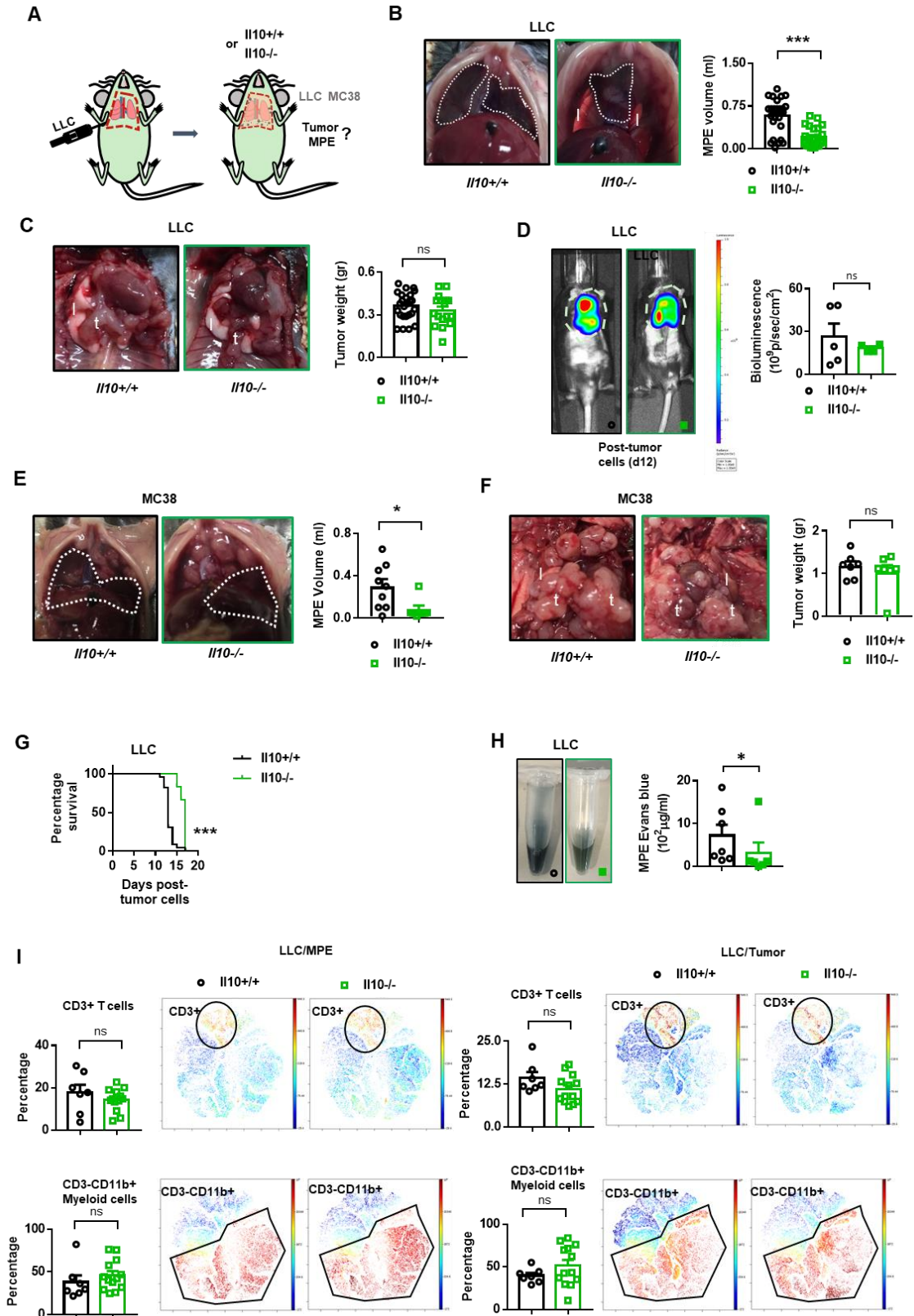


Figure 3.2. IL-10 deficient mice are protected in LLC/MC38-induced MPE.

(A). Scheme of the MPE model. MPE was induced via intrapleural injection of mice with cancer cell.

(B). MPE of either IL-10 KO mice and their littermate controls 14 days post intrapleural injection of LLC cells. Colored lines indicate mean MPE volumes caused by LLC cells. Representative images of MPEs (dashed lines) through the diaphragm.

(C). Pleural tumors of either IL-10 KO mice and their littermate controls 14 days post intrapleural injection of LLC cells. Colored lines indicate mean MPE volumes caused by LLC cells. Representative images of pleural tumors (t) and lungs (l) imaged through the diaphragm.

(D). Bioluminescent images of either IL-10 KO mice and their littermate controls were injected intrapleurally with 1.5×10^5 CAG.Luc.eGFP LLC cancer cells.

(E). MPE of either IL-10 KO mice and their littermate controls 14 days post intrapleural injection of MC38 cells. Colored lines indicate mean MPE volumes caused by MC38 cells. Representative images of MPEs (dashed lines), pleural tumors (t), lungs (l), and hearts (h) imaged through the diaphragm.

(F). Pleural tumors of either IL-10 KO mice and their littermate controls 14 days post intrapleural injection of MC38 cells.

(G). Comparison of overall survival of WT or IL-10 KO MPE mice with intrapleural injection of LLC cells (each $n = 20$).

(H). MPE-bearing mice received Evans' blue i.v. 1 h before sacrifice (day 14). Vascular permeability was assessed using the Miles assay. Pleural effusion was collected and quantification of Evans' blue leakage. Vascular permeability is abrogated in IL-10^{-/-} mice.

(I). viSNE analysis of CD3⁺ T cells and CD3⁺CD11b⁺ myeloid cells. Clustering is based on MFI of CD3 and CD11b. Black circle indicates IL-10 rich region. Data are representative of two independent experiments.

Data shown as mean \pm SEM. ns, * and ***: $p > 0.05$, < 0.05 , and < 0.001 , respectively.

The concentration of IL-10 is reported to be higher in human pleural effusion than in peripheral blood (Chen et al., 1996; Klimatsidas et al., 2012). However, little is known regarding whether IL-10 level is higher in human MPE compared to benign pleural effusion (BPE). Therefore, we measured IL-10 concentrations in parapneumonic pleural effusion (PPE) of 16 patients, in transudative pleural effusion (TrPE) of 17 patients, in lung cancer induced MPE of 18 patients and in other cancer induced MPE of 11 patients, and results are shown in **Figure 3.3**. The concentration of IL-10 in MPE is higher than in all the other test samples. These data suggest that IL-10 is participating the formation of inflammatory (exudative) effusions.

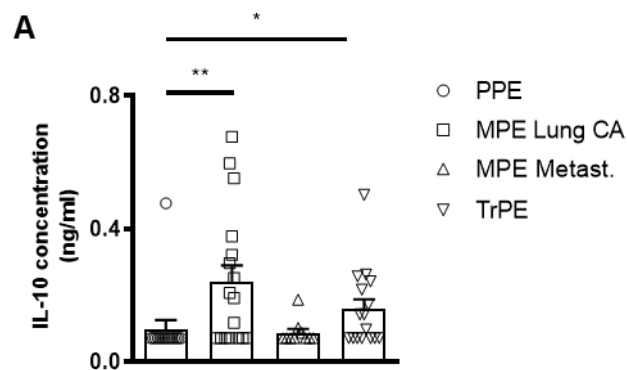


Figure 3.3. IL-10 concentration in benign and malignant pleural effusion of human.

(A). IL-10 concentration from parapneumonic pleural effusion (PPE) (n =16), MPE from lung cancer (n =18), MPE from other cancer (n=11) and Transudative pleural effusion (TrPE) (n =17) was quantified by ELISA.

Data shown as mean \pm SEM. Numbers in boxes refer to sample size. * and **: p <0.05 and <0.01, respectively.

3.3. Interleukin-10 mainly comes from myeloid cells.

Next, we wanted to check the cellular source of IL-10. We used IL-10^{eGFP} reporter mice (Tiger mice) (Kamanaka et al., 2006) and we detected the IL-10^{eGFP} expression in CD45⁺ cells isolated from LLC induced MPE as well as in

the pleural tumor by using FACS (**Figure 3.4 B; Figure 3.5 A**). Furthermore, we gated on CD45⁺IL10^{eGFP} cells and observed that IL-10^{eGFP} is mainly expressed in CD11b⁺ cells (90.83%±1.369), rather than CD3⁺ cells. We further validated these results, using a different reporter mouse - 10Bit mouse - as well as intracellular staining for IL-10 (**Figure 3.4 C; Figure 3.5 B**).

Previous studies showed that MPE formation was dominated by both polymorphonuclear and mononuclear myeloid cells that expressed both CD11b and Gr1, and either Ly6c or Ly6g (Agaloti et al., 2017). Therefore, within CD11b⁺IL-10^{eGFP} cells, we stained for Ly6c and Ly6g markers. Interestingly, we observed that the main source of IL-10^{eGFP} is CD11b⁺ Ly6c⁻ and Ly6g⁻ cells (**Figure 3.4 D**), which might be monocytes/macrophages (Rose et al., 2012). To better visualize of the cellular source of IL-10, we used the viSNE plot, IL-10^{eGFP} population and CD11b⁺ population are overlapping, while Ly6C and Ly6g cells are spatially distinct (**Figure 3.4 E; Figure 3.5 C**). In addition, there are some CD3⁺ cells also positive for IL-10^{eGFP}. Taken together, we revealed that myeloid cells, especially macrophages from the MPE of LLC-injected WT mice were the major cellular source of IL-10.

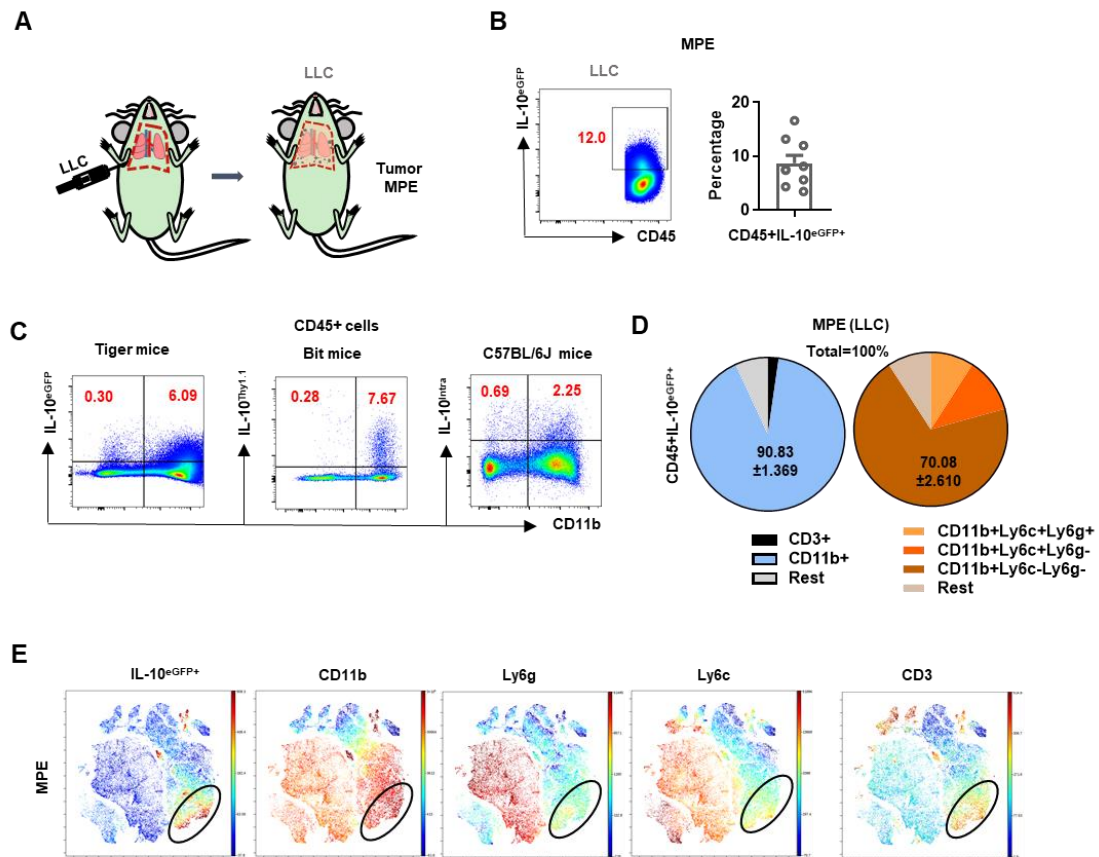


Figure 3.4. Interleukin-10 is highly secreted in MPE-competent model and mainly coming from myeloid cells.

(A). Scheme of the MPE model. MPE was induced via intrapleural injection of mice with cancer cell.

(B). IL-10^{eGFP} expression in LLC cells induced MPE.

(C). Representative FACS plot of IL-10^{eGFP} expression in Tiger mice, CD90.1 expression in 10Bit mice and IL10 intracellular staining of C57BL/6J mice.

(D). Source of IL10^{eGFP} in CD45⁺ cells (left) and CD11b⁺ cells (right).

(E). Visualization of t-distributed stochastic neighbor embedding (viSNE) analysis of IL-10^{eGFP}-producing CD45⁺ immune cells. Clustering is based on MFI of IL-10^{eGFP}, CD11b, Ly6g, Ly6c and CD3. Black circle indicates IL-10 rich region. Data are representative of two independent experiments.

Data shown as mean \pm SEM.

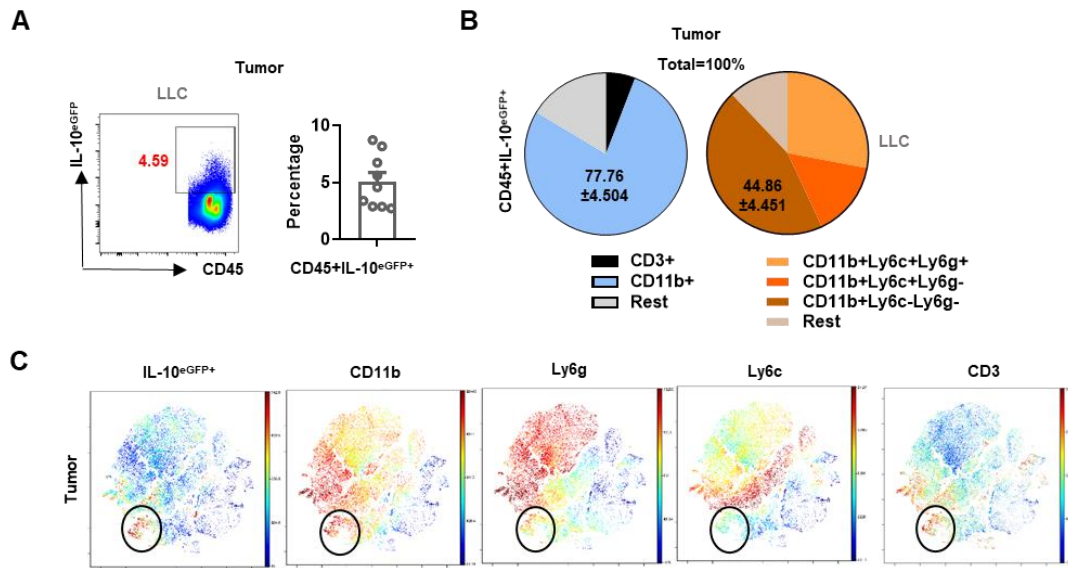


Figure 3.5. IL-10^{eGFP} expression in the tumor-infiltrating immune cells.

(A). Tumor-infiltrating immune cells (CD45⁺) IL-10^{eGFP} expression in MPE-competent and MPE-incompetent model.

(B). Source of IL10^{eGFP} in CD45⁺ cells (left) and CD11b⁺ cells (right).

(C). viSNE analysis of IL-10-producing CD45⁺ immune cells in tumors. Clustering is based on MFI of IL-10, CD11b, Ly6g, Ly6c and CD3. Black circle indicates IL-10 rich region. Data are representative of two independent experiments.

Data shown as mean \pm SEM.

3.4. The transcriptional landscape of myeloid cells in the MPE

Our data show that myeloid cells are the main population in the MPE environment, and also the main source of IL-10. Considering that monocyte/macrophages are a heterogeneous population, we performed single-cell RNA sequencing (scRNA-seq) technology in order to have an unsupervised characterization of these cells.

We isolated CD11b⁺ myeloid cells from MPE of LLC cell injected mice. We used these cells for scRNA-seq. In particular, we repeated this experiment twice using five mice in each experiment. We used “Harmony” and “Seurat” packages to combine the data of these two scRNA-seq data sets and using the same filtering

criteria, we captured 1989 cells (after filtering out low viability cells). The description of scRNA-seq quality controls is reported in **Table 3.1**. The data of the two scRNA-seq data sets were superimposable, suggesting that we can perform downstream analysis with the integrated data (**Figure 3.6 A**). The analysis clustered the cells into 8 discrete cell populations (**Figure 3.6 B**). Gene expression patterns of established canonical markers of immune cells allowed us to assign putative biological identities to each cluster that are described below, including macrophages (cluster 0, cluster 1, cluster 2 and cluster 3), dendritic cells (cluster 4), CD8 T cells (cluster 5), granulocytes (cluster 6) and B cells (cluster 7) (**Figure 3.6 B, D, E**). We found that *IL10* is mainly enriched in macrophage clusters, i.e. 0, 1, 2 and 3 (**Figure 3.6 B, C**).

Table 3.1. Quality control of alignment and summary of statistics from CellRanger.

Parameters	Sample 1	Sample 2
Estimated Number of Cells	1,141	2,908
Mean Reads per Cell	247,075	50,346
Median Genes per Cell	2,587	801
Number of Reads	281,912,899	146,407,457
Valid Barcodes	98.20%	98.00%
Sequencing Saturation	91.30%	73.40%
Q30 Bases in Barcode	97.80%	97.20%
Q30 Bases in RNA Read	89.30%	64.30%
Q30 Bases in Sample Index	96.50%	/
Q30 Bases in UMI	98.00%	97.30%
Reads Mapped to Genome	91.90%	90.00%
Reads Mapped Confidently to Genome	88.60%	87.30%
Reads Mapped Confidently to Intergenic Regions	5.10%	3.90%
Reads Mapped Confidently to Intronic Regions	13.40%	12.30%
Reads Mapped Confidently to Exonic Regions	70.00%	71.00%
Reads Mapped Confidently to Transcriptome	65.90%	67.10%
Reads Mapped Antisense to Gene	1.30%	1.00%
Fraction Reads in Cells	77.30%	86.30%
Total Genes Detected	13,778	14,843
Median UMI Counts per Cell	9,894	1,954

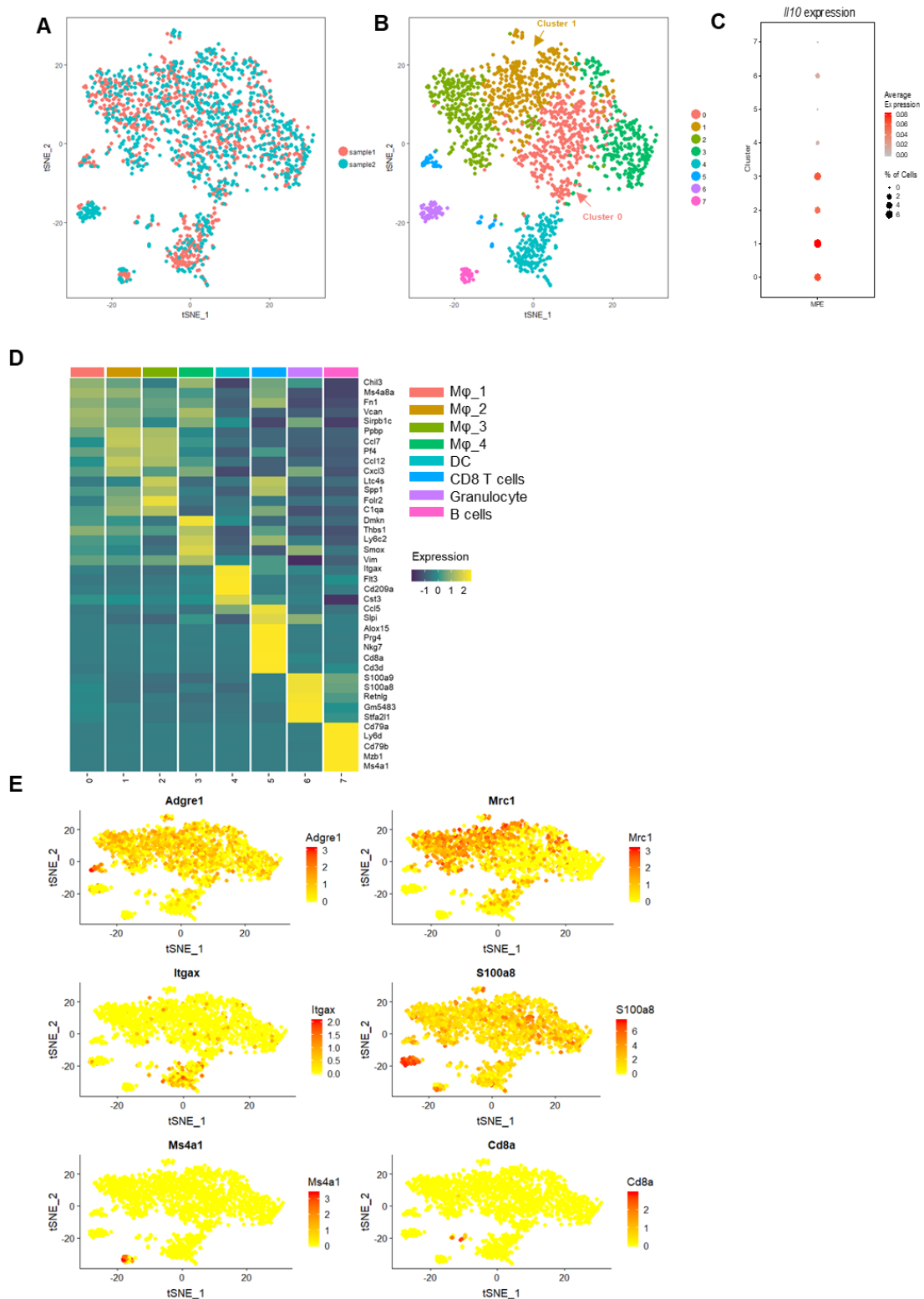


Figure 3.6. Identification of MPE-associated myeloid cell populations.

(A. B), t-Stochastic neighbor embedding (t-SNE) representation of aligned gene expression data in single cells extracted from murine MPE (n=1989). (A) Integrating two single cell RNA

sequencing, showing two experiments have the similar clusters. **(B)**. Different clusters in combined dataset, cell identities were assigned based on expression of canonical markers.

(C), *Ii10* mRNA expression level and percentage in each cluster.

(D), Heatmap showing the statistically upregulated genes (ordered by decreasing p value) in each cluster defined in **A** and selected enriched genes used for biological identification of each cluster (scale: log2 fold change).

(E), Gene expression patterns projected onto t-SNE plots of *Adgre1*, *Mrc1*, *Itgax*, *S100a8*, *Ms4a1* and *Cd8a* (scale: log-transformed gene expression).

We checked several typical macrophage genes, such as *Adgre1*, *Csf1r*, *Cd68*, *Fcgr1*, *F13a1* and *Lyz2* (**Figure 3.7**) in the macrophage clusters (cluster 0, 1, 2 and 3), and we use DC (cluster 4) as a negative control. These 4 macrophage populations expressed all the macrophage specific genes, while these genes in dendritic cells are significantly low expressed. This indicated that these four clusters represent indeed macrophages. However, it should be noted that most of these genes displayed heterogeneous or bimodal expression patterns within populations and an overlap between populations.

For example, *Csf1r* is significantly highly expressed in cluster 1, while *Fcgr1* is high in cluster 1 and cluster 3, and *Lyz2* overlapped between cluster 0 and cluster 3.

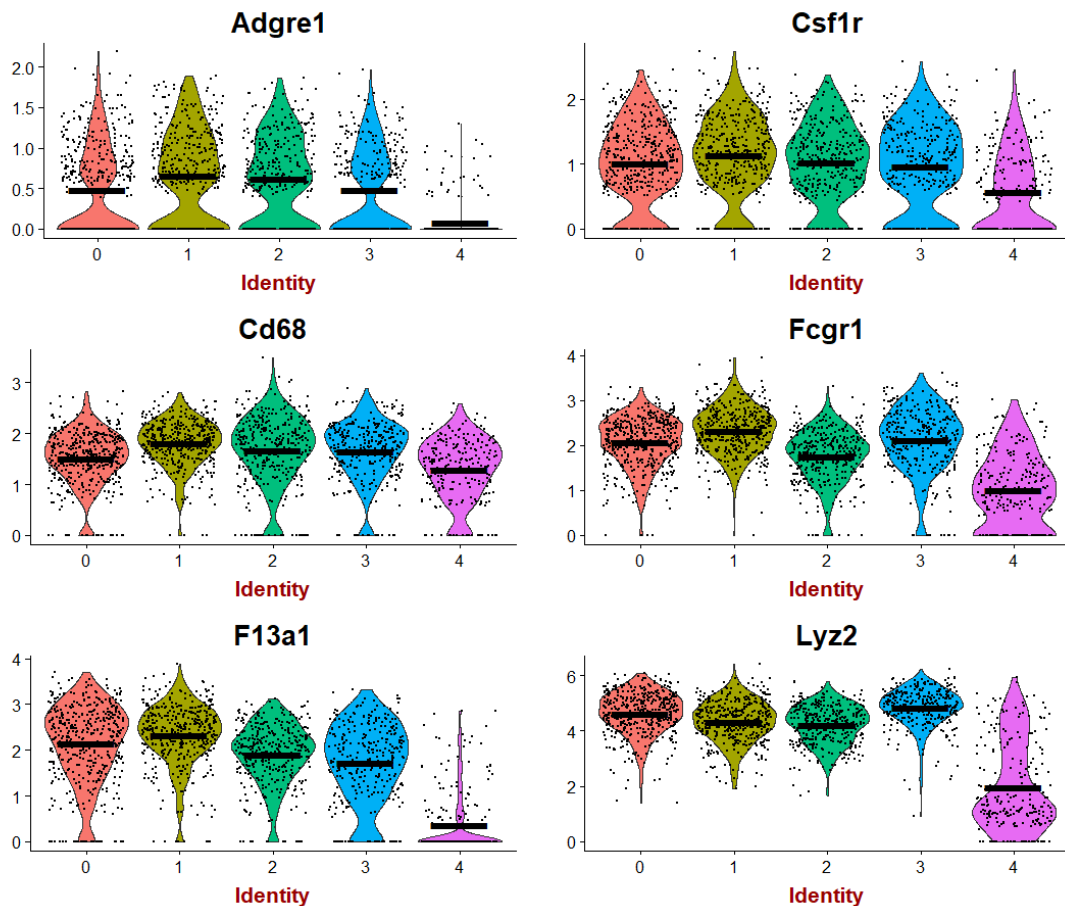


Figure 3.7. Violin plots of log-transformed gene expression of selected genes showing statistically significant upregulation in M ϕ .

To further understand the potential function of these 4 macrophage subsets found in MPE, we performed gene ontology (GO) term analyses on cluster 0, cluster 1, cluster 2 and cluster 3 (**Figure 3.8**). As expected for cells sharing a similar macrophage transcriptome, same biological processes like leukocyte migration, cytokine production and several metabolic processes were overlapping.

In particular, cluster 0 contains multiple transcripts related to metabolism, including cofactor (inorganic substances that are required for, or increase the rate of, catalysis), coenzyme (organic molecules that are required by certain enzymes to carry out catalysis), as well as many other metabolic processes, such as nicotinamide nucleotide metabolic process and pyridine nucleotide

metabolic process. The cells of cluster 0 expressed also many key genes associated with glycolysis genes, such as *Tpi1*, *Pgk1* (Penny et al., 2016), *Pkm* and *Ldha* (Karmaus et al., 2017), indicating that this cell cluster has a high metabolic activity.

Cluster 1 is enriched for genes including *Ppbb* (Smith et al., 2015) (also known as *Cxcl7*, a potent neutrophil chemoattractant and activator) and *Ccl2* (which could synergized with CXCL8 to promote neutrophil migration), all of which are critical for chemotaxis and leukocyte migration. Similar to cluster 1, cluster 2 is also enriched for genes associated with migration, such as *Pf4* (Lishko et al., 2018) (a heparin-binding protein with chemotactic activity for neutrophils and monocytes) and *Trem2* (Li et al., 2019) (reported to macrophage chemotaxis and phagocytosis). Those genes suggest a pro-migratory gene signatures of macrophages in an unresolved inflammation like MPE. In addition to leukocyte migration, cluster 2 gene expression also relates to epithelial proliferation, including genes like *Hmox1* (heme oxygenase-1), *Arg1* (arginase), *Gpx1* (Cheng et al., 2013) (glutathione peroxidase-1, a ubiquitously expressed antioxidant enzyme that scavenges organic hydroperoxides and protects cells from reactive oxygen species as well as hydrogen peroxide–induced or-dependent apoptotic injury, and promote epithelial proliferation). For example, macrophages can metabolize arginine to ornithine, a precursor of polyamine and hydroxyproline, and urea *via* Arginase (*Arg1*), which promotes wound healing, angiogenesis and tissue homoeostasis. These data suggest that Macrophages of cluster 2 can be involved in tissue remodeling especially of the vascular systems. Macrophage of cluster 3 are also enriched for genes that are involved in metabolism and cell migration, including genes (like *Fdps*, *Hmgcs1*, *Cyp51*, *Gch1* and *Sqle*).

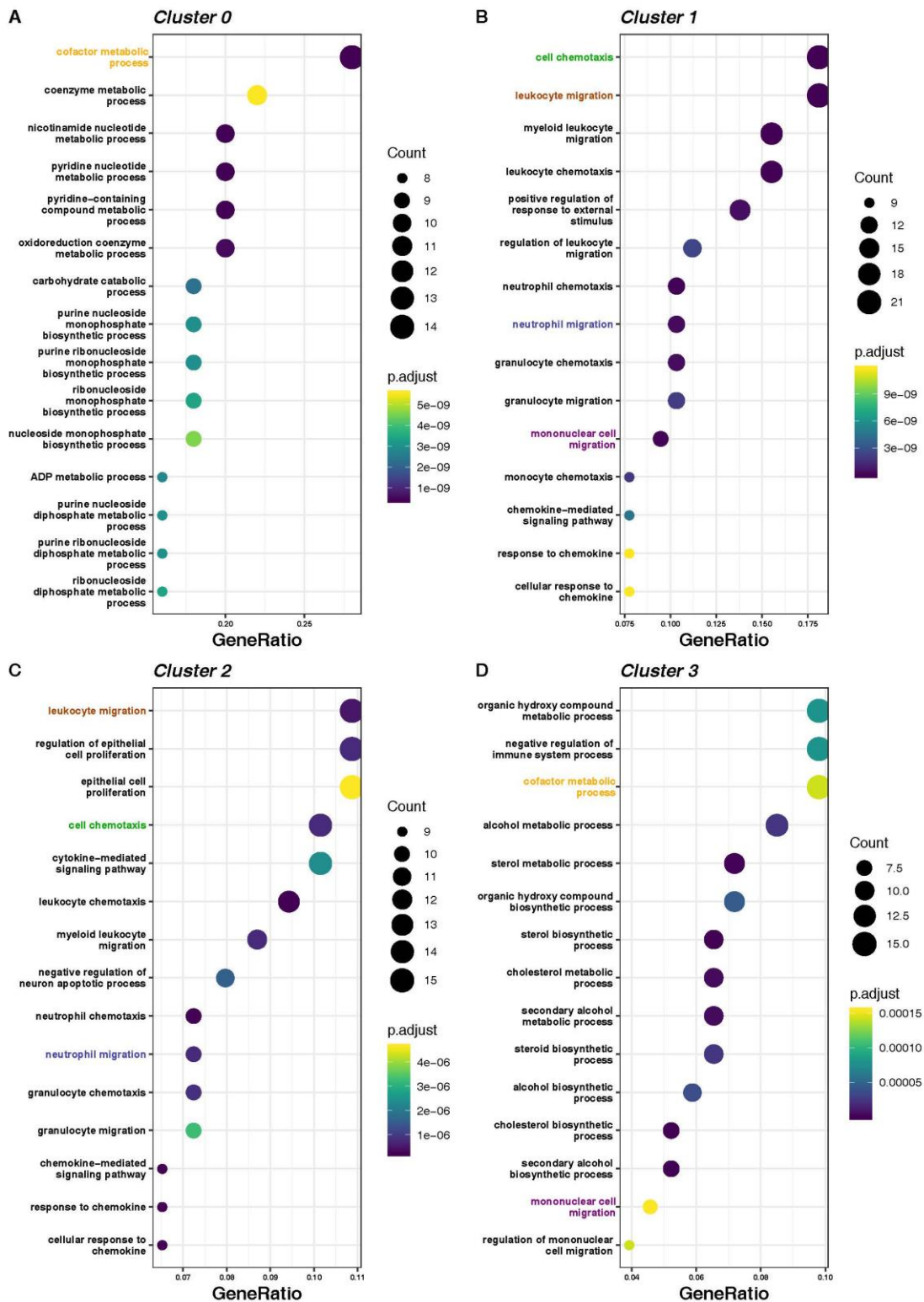


Figure 3.8. Top 15 terms identified by GO enrichment analyses for cluster 0, cluster 1, cluster 2 and cluster 3 plotted. Adjusted p value for each annotation is represented by color scale. Gene ratio is represented by dot size. Enriched terms were identified as significant at an adjusted p value ≤ 0.01 and FDR ≤ 0.05 .

VennDiagram of the differential expressed genes

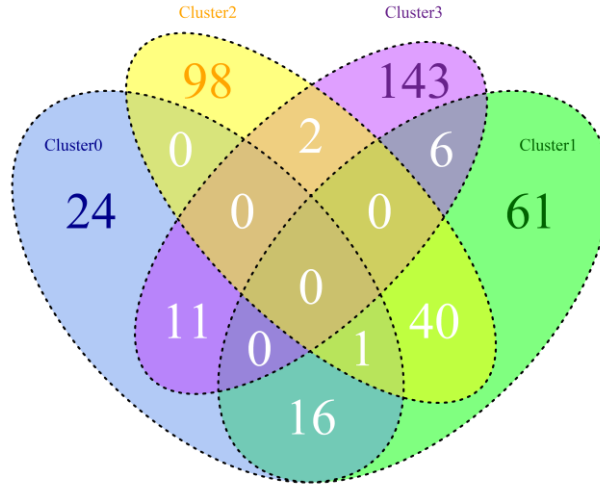


Figure 3.9. The Venn graph showing the overlap of differential expressed genes identified in different monocyte/macrophages clusters (cluster 0, cluster 1, cluster 2 and cluster 3).

Table 3.2. Distinct genes in each cluster from the VennDiagram

Cluster 0	Cluster 1		Cluster 2		Cluster 3		
Fn1	Cxcl3	Rab1a	Ltc4s	Mpp1	Dmkn	Selk	Prdx6
Sirpb1c	Ccl2	Clta	Spp1	Mrps28	Ly6c2	Cytip	Arf5
Ccr2	Aif1	Zeb2	Folr2	Glul	Smox	Gyg	Rnf149
Gm9733	Ms4a6d	H1f0	Cbr2	Ndufa12	Vim	Glrx	Uqcrh
Il1r2	Snx6	Pira2	Tmem37	Lifr	Fdps	Uck2	Creld2
Emb	Dab2	Pdia3	Emp1	Bax	Mgst1	Pfkp	Map2k3
Pirb	Ms4a6b	Npc2	Gpx1	Ap2m1	Actg1	Anxa1	Fam49b
Fos	Gja1	2610001J05Rik	Trem2	Nhp2	Tgm2	Coro1a	Phlda1
Igsf6	Msr1	Nt5dc2	Lmna	Hnrnpab	Cd44	Ldlr	Mpc1
Ncf4	Snx5	Vmp1	Wfdc17	Dcxr	Clec4e	Insig1	Ppp2ca
Prtn3	Il4ra	Lrrc25	Klf2	Hsp90ab1	Adam8	Ncf2	Arf4
AW112010	Fcgr2b	Akr1a1	Mt2	Wnk1	Tgfb1	Ramp1	Lgals8
Bnip3	Rab3il1		Lpl	Vat1	Plac8	Osm	Sec23b
Pgd	Itm2b		Timp2	Rhoc	Msmo1	Lyn	Lilr4b
Pgam1	Ms4a6c		Emp3	Ndufc1	Hmgcs1	Slc15a3	Ufm1
C1rl	Tmem261		Crip1	Add3	Mmp8	Cebpb	Rhov
Dpep2	Marcks1		Cdkn1a	Atp5g1	Clec4d	Marcks	Rbms1
Smim4	Nxpe5		Metrn1	Pltp	Aldh2	Irf5	Srgn
S100a11	Rnpep		Cd36	Wwp1	Tpm4	Anxa2	Chmp4b
Prdx5	AF251705		Sdc3	Flna	Taldo1	Cndp2	Rplp0
Csf2ra	Hk3		Rps271	Park7	Pyhin1	Jarid2	Por
Adssl1	Anxa3		Ninj1	Rexo2	Samhd1	Sc5d	Sifn2

Cyp4f18	Lst1	Hint1	Cd93	Idi1	H2afj	Uba52
Slc7a11	Ap2s1	Tbxas1	Nme1	Cyp51	Fgl2	Uqcrfs1
	Rab5c	Tppp3	Ran	Lilrb4a	Atf3	Ptpn1
	Calr	Lrp1	Timm13	Ifitm6	Rpl10	Hmgcr
	Tmem106a	Bri3	S100a10	Lrrfip1	Gstm1	Atp6v1a
	Adap2	Naaa	Uap111	Rnh1	Mpeg1	Eif3f
	Clec4a1	Tubb2a	Frmd4b	Tpd52	Diaph1	Fyb
	Cd38	Rhob	Camk1	Esd	Sfn5	Sec61g
	Fcgr3	Pepd	Uqcr11	Mnda	Nab1	Plin2
	Slc3a2	Stab1	Fam20a	Cd177	Plaur	Kdm7a
	Rgl1	Ppp1r14b	Cycs	Evl	Clec5a	Rpl36al
	Ctsd	Ehd4	Mtss1	Nampt	Hspa8	Hnrnp2
	Ccr5	Mrpl23	Stom	Cd14	Capza2	Sec61b
	Lair1	Bola2	Anxa4	Mmp19	Filip1l	Ankrd37
	App	Fcgrt	Polr2f	Emilin2	Slc2a1	Tifab
	Pdia4	Dhrs3	Plec	Gch1	Psap	Krtcap2
	Tmem165	Prdx1	Gm10116	Lcn2	Trafd1	Fmn1l
	Ltb4r1	Klf4	Fth1	Slc16a3	Ccr1	Etf1
	Cyfp1	Ranbp1	Ptafr	Lsp1	Tarm1	Id2
	Rtp4	Atp1b3	Psma6	Napsa	Casp6	Cd86
	Lamp1	Ap1b1	Kras	Lgals3	Fam129b	Emd
	Nipa2	Hspe1	Ndufb8	Eif1	Al662270	Gk
	P2rx4	Slc28a2	Ppia	Sqle	Scp2	Ap3s1
	Cfp	Slc48a1	Mt1	Hif1a	Agpat9	
	Ehd1	Ms4a7	Rps26	Msrb1	Btg1	
	Slc11a1	Adam15	Atpif1	Manf	Gpr141	
	Hacd4	BC005537	Txndc17	Hspa5	S100a4	

Next, we wanted to understand what distinguishes these different populations of macrophages from each other. To this end, we used a Venn graph to check the distinct genes in each cluster (**Figure 3.9**). We got several differential expressed genes restricted to each cluster (24 genes for Cluster 0, 61 genes for Cluster 1, 98 genes for Cluster 2 and 143 genes for Cluster 3) (**Table 3.2**).

The cells of the cluster 0 expressed several genes, which are characteristically expressed by alternatively activated (M2) macrophages, including *Fn1*, *Ccr2* and *Il1r2*. For example, the anti-inflammatory IL-1 decoy receptor, *Il1r2*, has recently been shown to be elevated in plasma during sepsis (Giri et al., 1994), as well as a mouse model of chemically-induced lung injury (Martin et al., 2013) and human

lung disease, specifically acute respiratory distress syndrome (Kovach et al., 2015). Here, we think that the expression of *Ilr2* might be associated with MPE formation. Furthermore, the cells of the cluster 0 are highly enriched for *Ccr2* (which encode the cognate receptor of CCL2) (Zlotnik and Yoshie, 2012). Agaloti et al. (Agaloti et al., 2017) showed that *Ccr2* deficient mice were protected against MPE, suggesting that tumor cells drive MPE development via systemic CCL2 signaling to CCR2⁺ host cells.

Interestingly, the cells of the cluster 1 also showed an alternatively activated (M2) macrophages phenotype, which was reported to be induced by the signalling downstream of interleukin-4 receptor(R)a (Mauer et al., 2014). The cells of the cluster 1 expressed the pro-angiogenic cytokine *Cxcl3*, which was reported in benign pleural effusion. The cells of the cluster 1 also expressed sorting nexin (SNX) genes, including *Snx5* and *Snx6*, which might be associated with micropinocytosis, a key biological process which mediates the bulk endocytosis of solute molecules, nutrients and antigens (Lim et al., 2012). Both the cells of the cluster 0 and cluster 1 are involved in the secretion of chemokines (including genes *Ccl7*, *Ccl12* and *Ccl24*) (Owen and Mohamadzadeh, 2013).

The cells of the cluster 2 are characterized by the expression of *Trem2* (encoding triggering receptor expressed on myeloid cells 2). Deming et al. (Yuetiva Deming, 2018) reported that membrane-spanning 4-domains subfamily A (Ms4a) gene cluster is a key regulator of soluble Trem2, consistently, in our data, we found several Ms4a genes in the cells of cluster 1, such as *Ms4a6b*, *Ms4a6c* and *Ms4a6d*. This might suggest a possible interaction between the cells of cluster 1 and cluster 2. Notably, the cells of the cluster 2 produce *Spp1* (encode osteopontin). *Spp1* was identified as a key mediator of vascular permeability that leads to MPE accumulation (Psallidas et al., 2013). In addition to its vasoactive effects, tumor-secreted *Spp1* can cause mast cell activation and degranulation (Giannou et al., 2015). Collectively, our data suggest that macrophages could

also produce *Spp1* during MPE development. In addition, the cells of the cluster 2 showed genes that were reported to be in both alveolar macrophages and interstitial macrophages, like LTC4 synthase (*Ltc4s*), and *Emp1*, which was reported in interstitial macrophages. As the cells of the cluster 2 showed some expression of these markers, no clear patterns emerged that could allow us to assign this population to previously proposed macrophage subsets.

The cells of the cluster 3 are selectively characterized by *Ly6c2* and *Cd14*. *Cd14* is strongly expressed in monocytes and in most tissue macrophages, therefore, the cells of the cluster 3 might be a monocyte identity. The cells of this cluster are enriched for *Dmkn*, a gene differentially upregulated in inflammatory conditions, and whose role was defined in the early endocytic pathway (Naso et al., 2007).

Taken together, these data illustrate heterogeneity within the myeloid cells in MPE that was never revealed before and that could help to understand the potential different function of these macrophages clusters.

3.4.1 The functional state of the macrophages

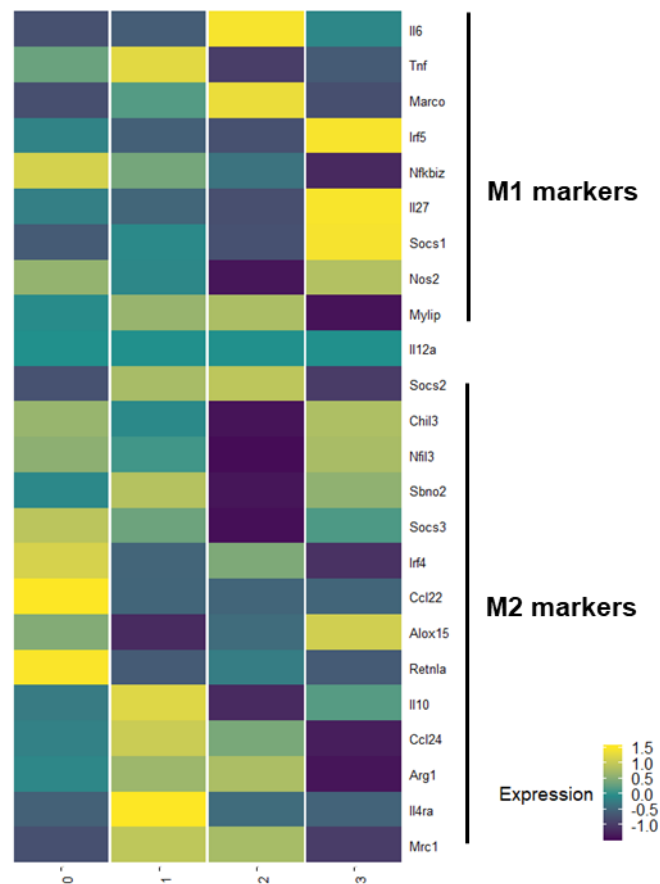


Figure 3.10. Expression of consensus M1/M2 markers in different clusters. Top panel – M1 markers; Bottom panel – M2 markers.

Macrophages with different program states (i.e., proinflammatory or tissue remodeling, classical or alternative, or “M1” versus “M2” like) are commonly considered to populate malignant pleural effusion. We, therefore, investigated whether the 4 clusters reported here could be defined based on the expression patterns of typical macrophage markers (**Figure 3.10**). Both cluster 0 and cluster 1 showed an alternative activated macrophage phenotype, including *Mrc1* (encoding the mannose receptor, CD206), *Ccl2*, *Il4ra* and *Il10* (Poczobutt et al., 2016). The expression level of IL-10 between cluster 0 and cluster 1 was comparable, indicating that these two clusters are the source of IL-10. However,

there were no clear distinction between cluster 2 and cluster 3 for these types of programming markers.

Besides the 4 clusters of macrophages, other cell populations were identified, including a granulocyte cluster (cluster 6; eg, enriched genes: *S100a8* and *S100a9*), a B cells cluster (cluster 7; eg, enriched genes: *Cd79a*, *Cd79b*, *Ly6d*, and *Mzb1*) and a T cells cluster (cluster 5; eg, enriched genes: *Cd3d* and *Cd8a*), considering their low *Itgam* (*Cd11b*) expression in B cells cluster and T cells cluster, these two clusters might be due to sorting contamination.

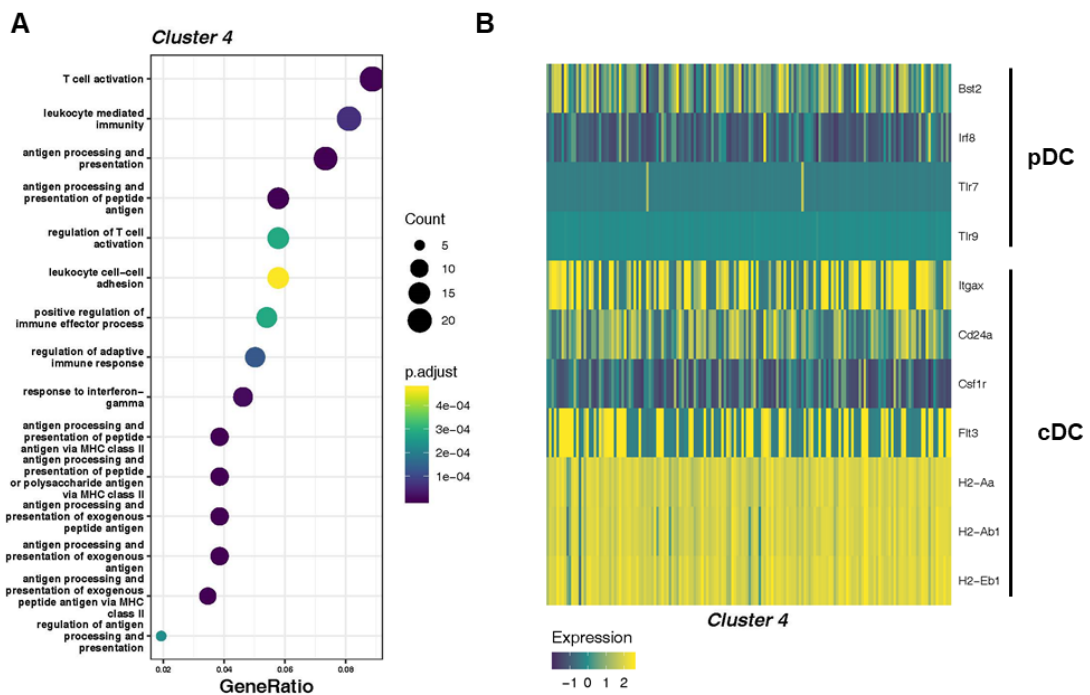


Figure 3.11. (A) Top 15 terms identified by GO enrichment analyses for cluster 2 plotted. Adjusted p value for each annotation is represented by color scale. Gene ratio is represented by dot size. Enriched terms were identified as significant at an adjusted p value ≤ 0.01 and FDR ≤ 0.05 . (B). Heatmap of the DC associated genes.

Finally, we identified a cluster of dendritic cells (cluster 4; *Itgax*, *Cd209a*). Dendritic cell cluster comprised MHC (major histocompatibility complex) class II-related genes (*H2-Aa*, *H2-Ab1*, and *H2-Eb1*). In addition, dendritic cell cluster is

enriched for expected biological processes such as T-cell activation, antigen processing and presentation through MHC class II (**Figure 3.11 A**). We next wondered whether they are plasmacytoid dendritic cells (*Clec4c*, *Tcl1a*, *Irf8* and *Tlr7*) or conventional dendritic cells (*Cd11b*, *Itgax*, *Cd24a*, *Cd115*, *Flt3* and MHC Class II-related genes). The expression pattern of these cells indicated that they are more likely conventional dendritic cells (**Figure 3.11 B**).

3.5. The driving factor for the IL-10 secretion.

How IL-10 is induced in MPE microenvironment is still unclear. Compared with peripheral blood, we detected more apoptotic cells in the pleural effusion (**Figure 3.12 A**), and the apoptotic cells are mainly CD45⁺ immune cells (**Figure 3.12 B**). Macrophages can recognize apoptotic cells by sensing phosphatidylserine (PtdSer) (Fadok et al., 1992; Poon et al., 2014; Savill et al., 1989). The PtdSer-dependent receptor tyrosine kinases (RTKs) AXL and MERTK, can be found in both BMDMs (Zagorska et al., 2014), tissue-resident macrophages (Gautier et al., 2012; Zagorska et al., 2014), and in macrophages from MPE (**Figure 3.12 C, D**). These receptors are fundamental for the phagocytosis of apoptotic cells (Rothlin et al., 2015). Therefore, it is reasonable to propose that macrophages in MPE sense and phagocyte the apoptotic cells through Axl and Mertk receptors and in turn produce IL-10.

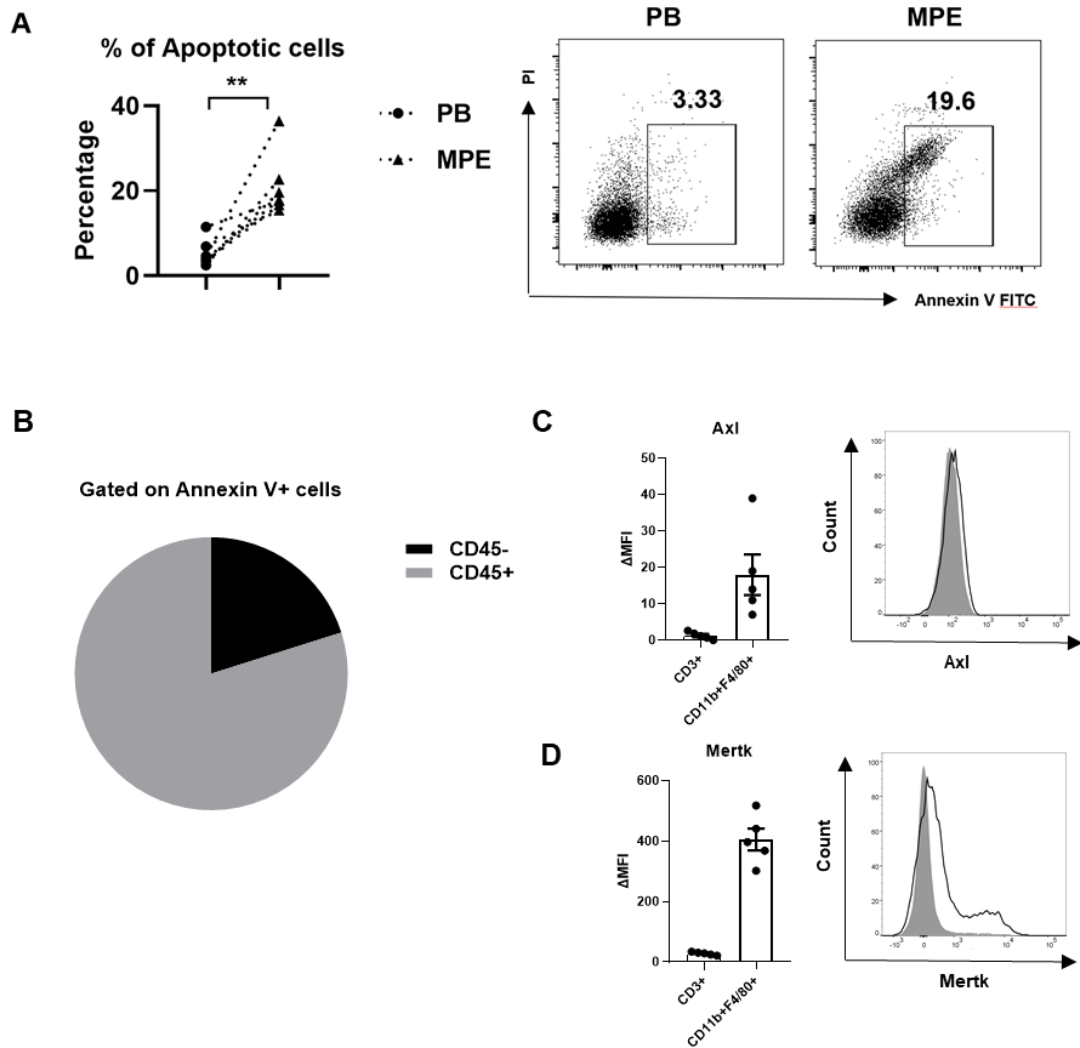


Figure 3.12. Macrophages expressed AXL and MERTK receptors to phagocytose the apoptosis cells in MPE.

(A). Apoptosis rate in cells in peripheral blood and MPE was assessed by flow cytometry using the Ann-V/propidium iodide (PI) apoptosis assay. (Left) Percentage. (Right) Representative dot plot showing frequency of early/late apoptotic cells.

(B). Different cell types (Based on the expression of leukocyte common antigen (CD45)) were gated on Annexin V⁺ apoptotic cells.

(C, D). Levels of expression of Axl receptor (C) and Mertk receptor (D) on CD11b⁺F4/80⁺ (Macrophages) and CD3⁺ (T cells) immune cells in MPE. (Left) Dot plots showing the delta mean fluorescence intensities (Δ MFI) of Axl receptor and Mertk receptor on Macrophages and T cells relative to that of FMO controls from murine MPE. (Right) Flow cytometric histogram graphs showing a representative example from CD11b⁺F4/80⁺ (Macrophages) expressing Axl receptor

(C) and Mertk receptor (D) (The black open histogram) compared to FMO control (The filled gray histogram).

3.6. The target cells of IL-10 in MPE.

In order to know how IL-10 promotes MPE formation, we aimed to find the target cells of IL-10 in MPE. There are several possible candidate cell populations which could express IL-10 receptors, including cancer cells, Tregs, dendritic cells and macrophages.

We checked *Il10ra* (*IL10R1*) and *Il10rb* (*IL10R2*) gene expression in cultured LLC and MC38 cells. *Il10ra* gene is not detectable in those cancer cells, while *Il10rb* is ubiquitously expressed (Gibbs and Pennica, 1997; Lutfalla et al., 1993) (**Figure 3.13 A**).

We also checked IL10RA expression by FACS on the immune cells. Firstly, as a proof-of-concept experiment and to avoid the potential bias of an inflammatory environment, we isolated CD45⁺ and CD31⁺ cells from the lungs of mice under steady state, and stained for IL-10RA antibody. MFI of IL-10RA were significantly higher in CD45⁺ cells than CD31⁺ cells, indicating that the immune cells are more likely the target cells of IL-10 (**Figure 3.13 B**).

Secondly, although the above-mentioned CD45⁺ and CD31⁺ cells expressed IL-10 receptors, we next examined whether they can respond to IL-10. Therefore, we isolated CD45⁺ immune cells and CD31⁺ endothelial cells from mice under steady-state to test their responsiveness to IL-10. STAT3 can be activated by a variety of cytokines such as IL-6 and IL-10 (Finbloom and Winestock, 1995; Heinrich et al., 1998; O'Farrell et al., 1998). The peak of STAT3 phosphorylation (pSTAT3) occurs within 15 to 60 minutes after cytokine stimulation. After the peak, STAT3 activation continues to attenuate (Siveen et al., 2014). To determine if immune cells and endothelial cells were undergoing IL-10 signaling, the pSTAT3 was tested by flow cytometry. CD45⁺ and CD31⁺ cells pulsed with

recombinant IL-6 protein (100 ng/ml) and recombinant IL-10 protein (100 ng/ml) for 20 minutes demonstrated a significant increase in pSTAT3 staining compared to PBS treated cells (**Figure 3.14 A**), confirming that IL-10 signaling in CD45⁺ immune cells results in pSTAT3. CD3⁻ cells demonstrated a significant increase in pSTAT3 staining compared to PBS treated cells (**Figure 3.14 A**). CD31⁺ endothelial cells did not respond to either IL-6 or IL-10. The steady state results showed that IL-10 receptor is mostly expressed on CD3⁻ cells.

The next step will be to check IL-10 receptor expression under MPE condition. In addition, we plan to use a variety of mouse strains expressing Cre recombinase under the control of different cell-specific promoters, including Cdh5-Cre (endothelial cells), Lysm-Cre (neutrophils and macrophages) and CD11c-Cre (dendritic cells), and cross each Cre strain to *Il10ra*^{fllox/fllox} mice to get *Il10ra* conditional knockout mice.

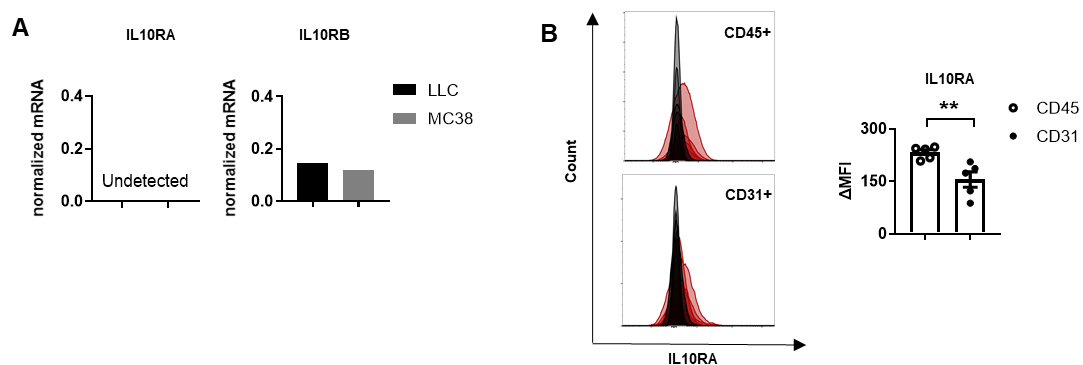


Figure 3.13. IL-10 receptor expression on cancer cell lines, immune cells and endothelial cells.

(A). qPCR detection of *Il10ra* gene (left) and *Il10rb* (right) expression in LLC and MC38 cancer cell lines.

(B). Concatenated FACS histogram showing superimposed IL-10ra expression in CD45⁺ cells (upper left) and CD31⁺ cells (lower left) from steady-state mice (n = 5). The right-hand column chart demonstrates IL-10ra expression (Delta geometric mean fluorescence intensity: deduce by the IL-10ra expression of isotype control) for each group (mean ± SEM).

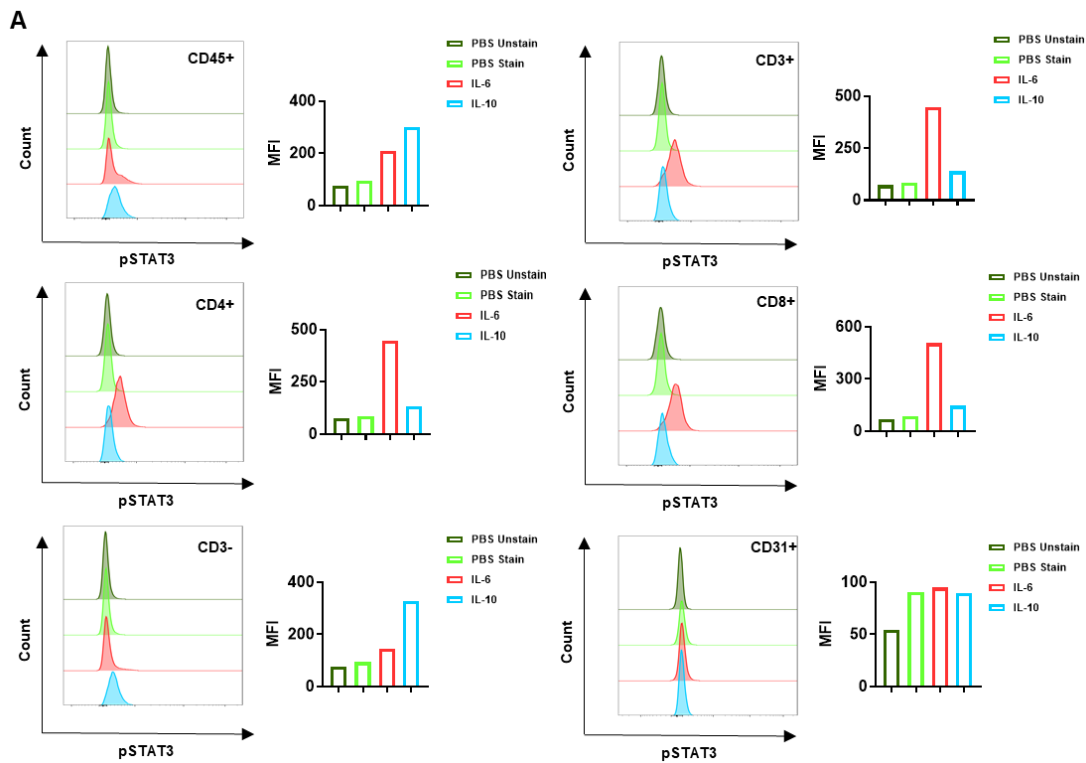


Figure 3.14. Heterogeneous STAT3 activation of different cells after IL-10 stimulation.

(A) pSTAT3 expression of live CD45⁺, CD3⁺, CD4⁺, CD8⁺, CD3⁻ and CD31⁺ cells cultured under various conditions (adding PBS, adding PBS but without antibody staining, adding IL-6 [100 ng/ml] and adding IL-10 [100 ng/ml]), as shown by representative histograms (left panel), summary bar graph of MFI (right panel).

3.7. Dendritic cells derived Timp1 could promote MPE.

Considering that *Il10ra* is mostly expressed on CD3⁻ cells under steady state conditions, and CD3⁻CD11b⁺ myeloid cells are the major population of the CD45⁺ immune cells in MPE, we checked the *Il10ra* expression in the scRNA-seq data from CD11c⁺ cells in MPE. DCs showed the highest *Il10ra* (Figure 3.15) compared with other cells, indicating that DCs might respond to IL-10 during the development of MPE.

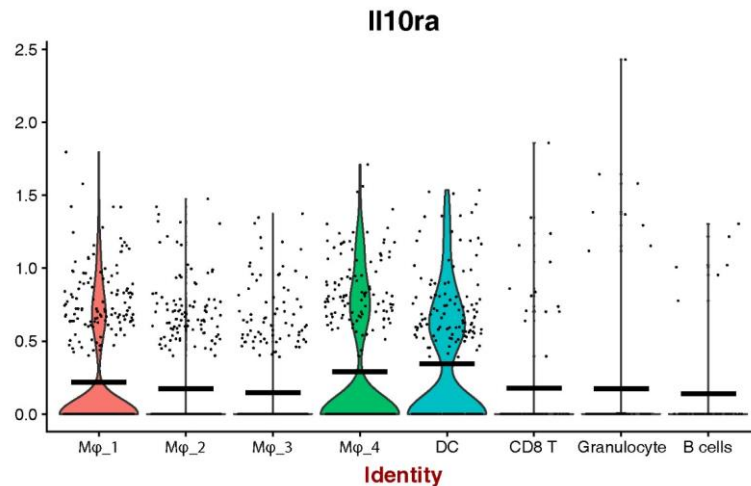


Figure 3.15. Violin plots of log-transformed gene expression of *Il10ra* gene in CD11b+ cells from scRNA-seq.

Interestingly, in our scRNA-seq data, *Timp1* is significantly enriched in DC compared to all the other populations (**Figure 3.16**). TIMP1 is a glycoprotein that regulates the structure of the extracellular matrix. Previous studies have reported a link between TIMP1 and angiogenesis. Tumors overexpressing TIMP1 showed increased expression of VEGF-A (Cui et al., 2015), increased growth rate with higher vascular density (Rojiani et al., 2015), and metastatic colonization in a mouse model of lung cancer (Chang et al., 2015). We next sought to determine whether DCs could be induced by IL-10 to express *Timp1*. To test this, we checked two different GSE dataset, we found that IL-10 induces *Timp1* expression in *in vitro* culture DC. *Timp1* expression increases and becomes more significant in human moDC culture with IL-10 (**Figure 3.17 A**. GSE45466). In addition, another dataset showed that *Timp1* is higher in human immature moDC and immature IL-10 APC (**Figure 3.17 B**. GSE92852).

Using publicly available GTEx normal tissue data (Consortium, 2013) (<https://www.gtexportal.org/>), we analyzed *Timp1* expression in various normal tissues. Both in human (**Figure 3.18 A**) and mouse (**Figure 3.18 B**), *Timp1* is expressed in all the tissues sampled, but strongly expressed in the lung, with the

lowest expression level in the bone marrow. Considering the abundant expression of Timp1 in both human and mouse lung tissue as well as the important role of Timp1 in cancer development, our data support a protumorigenic and prometastatic role for DC derived TIMP1 *via* alteration of tissue remodeling and the possible promotion of angiogenesis.

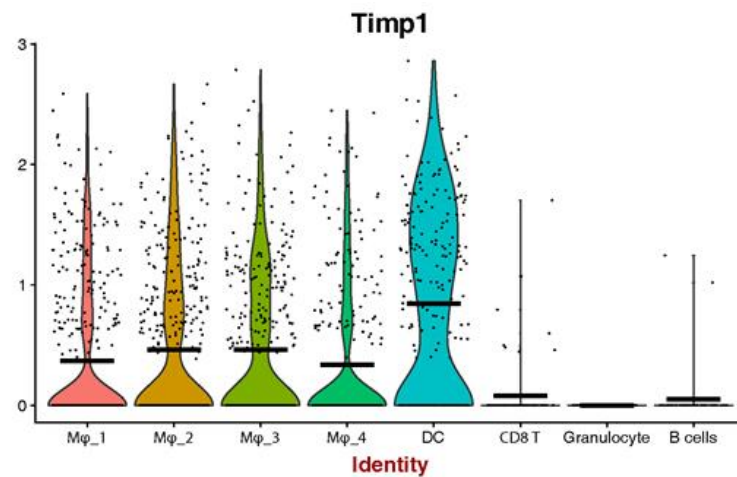


Figure 3.16. Violin plots of log-transformed *Timp1* gene expression in each CD11b⁺ population and showing significant upregulation in DC.

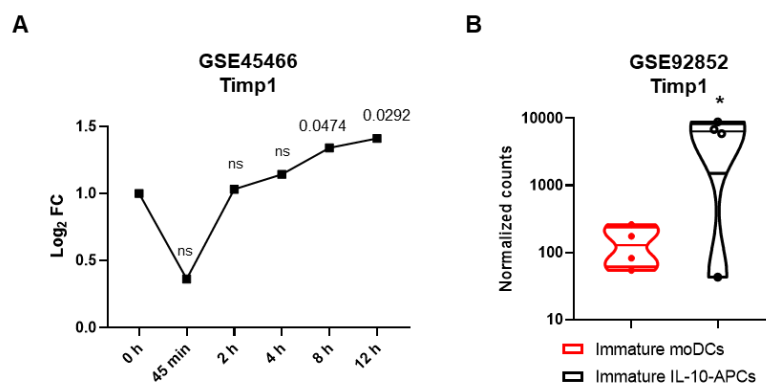


Figure 3.17. IL-10 induced DC producing Timp1.

(A). The expression levels of Timp1 in human moDC culture with IL-10 for 0 hour, 45 min, 2 hour, 4 hour or 8 hour from GSE45466 dataset. Above the bar shows the p value or ns (not significant) compared with the 0 hour.

(B). The expression levels (counts per million, CPM) of *Timp1* in human immature moDC and immature IL-10 APC from GSE92852 dataset ($p < 0.05$).

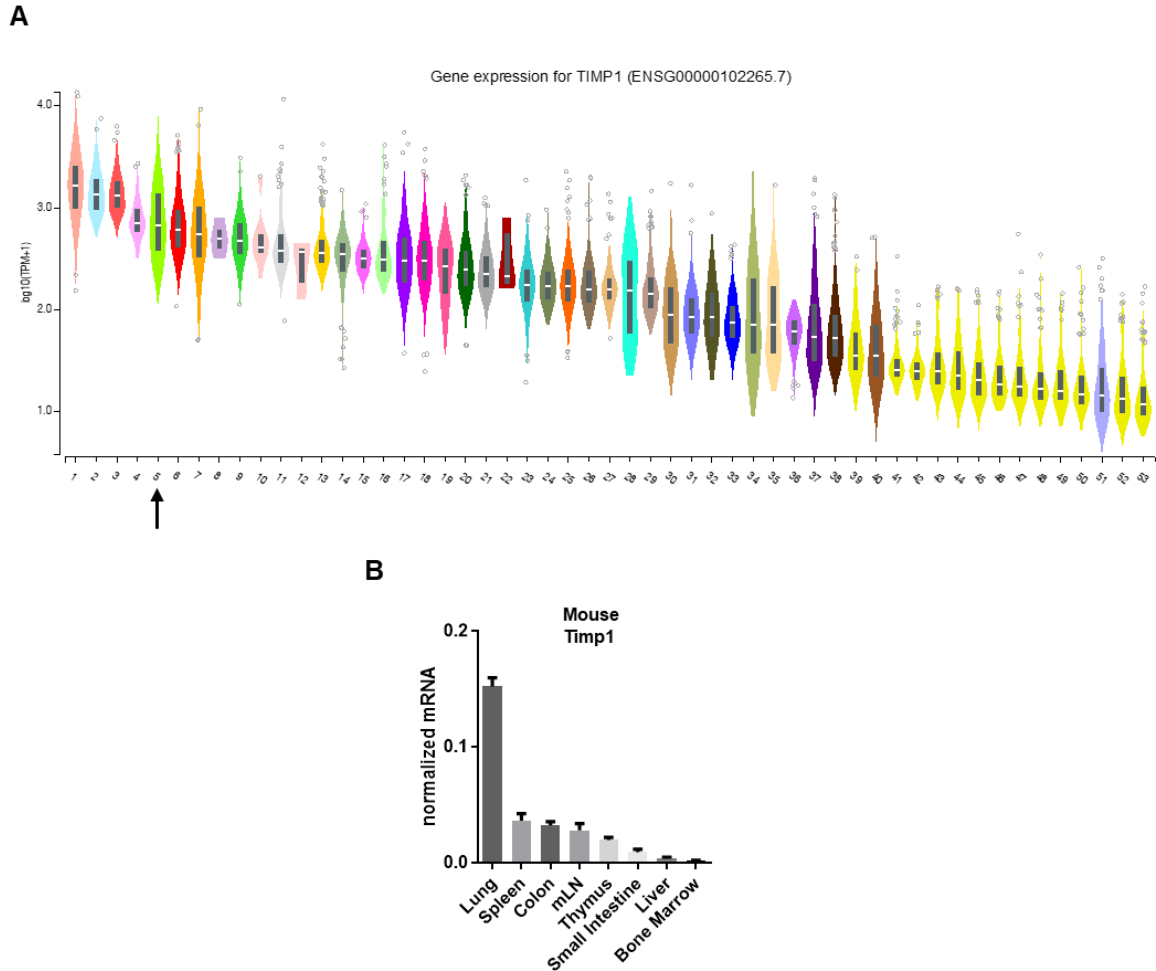


Figure 3.18. *Timp1* is enriched in the lung tissue.

(A). *Timp1* expression in normal human tissues. Expression of *Timp1* is shown for GTEx normal tissues. Tissue types were sorted by median expression of samples. Arrow indicates lung tissue. Serial number and corresponding tissue names are shown in **Table 3.3**.

(B). Tissue distribution of *Timp1* expression in steady-state mice. Expression of mice *Timp1* in different organs as detected by real-time PCR. Gene expression data were normalized to *Hprt* expression. Bar represents the mean \pm SEM ($n = 3$).

Table 3.3. Serial numbers shown in Figure 3.18 corresponding to the tissue types.

1	Artery - Coronary	28	Kidney - Cortex
2	Cells - Transformed fibroblasts	29	Esophagus - Muscularis
3	Artery - Aorta	30	Colon - Transverse
4	Ovary	31	Skin - Sun Exposed (Lower leg)
5	Lung	32	Small Intestine - Terminal Ileum
6	Artery - Tibial	33	Skin - Not Sun Exposed (Suprapubic)
7	Adipose - Visceral (Omentum)	34	Liver
8	Cervix - Endocervix	35	Stomach
9	Adrenal Gland	36	Cells - EBV-transformed lymphocytes
10	Fallopian Tube	37	Heart - Left Ventricle
11	Prostate	38	Esophagus - Mucosa
12	Cervix - Ectocervix	39	Brain - Spinal cord (cervical c-1)
13	Nerve - Tibial	40	Pancreas
14	Minor Salivary Gland	41	Brain - Cerebellum
15	Uterus	42	Brain - Cerebellar Hemisphere
16	Pituitary	43	Brain - Substantia nigra
17	Heart - Atrial Appendage	44	Brain - Hypothalamus
18	Whole Blood	45	Brain - Amygdala
19	Vagina	46	Brain - Nucleus accumbens (basal ganglia)
20	Thyroid	47	Brain - Caudate (basal ganglia)
21	Testis	48	Brain - Putamen (basal ganglia)
22	Bladder	49	Brain - Hippocampus
23	Breast - Mammary Tissue	50	Brain - Anterior cingulate cortex (BA24)
24	Spleen	51	Muscle - Skeletal
25	Adipose - Subcutaneous	52	Brain - Cortex
26	Esophagus - Gastroesophageal Junction	53	Brain - Frontal Cortex (BA9)
27	Colon - Sigmoid		

3.8. Working hypothesis of IL-10 promoting MPE.

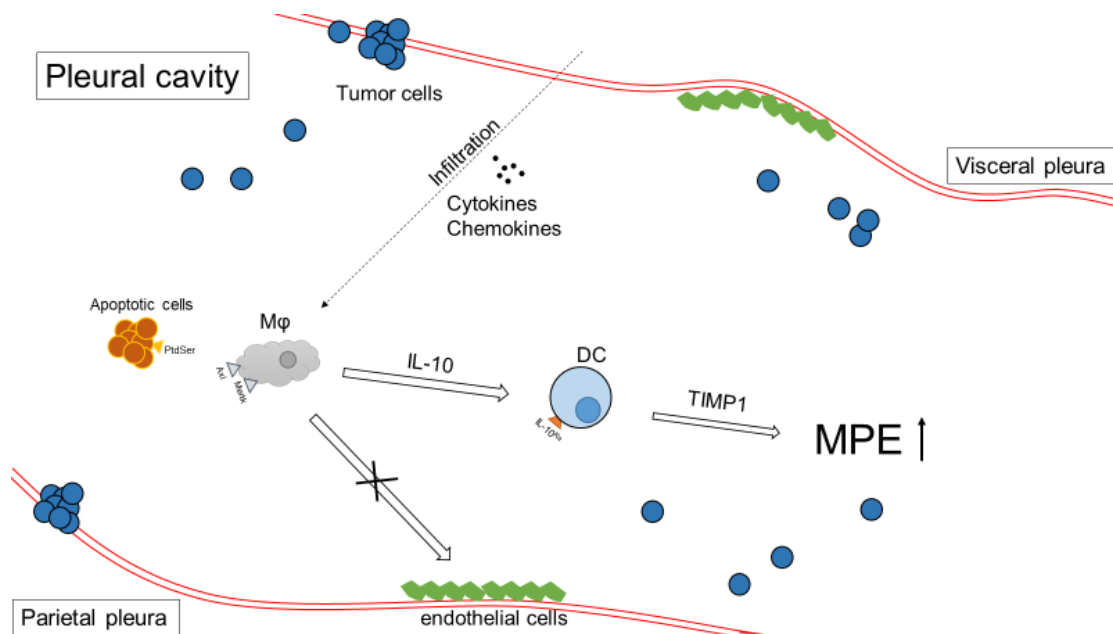


Figure 3.19. Working hypothesis: Macrophages produce IL-10 and promote MPE by activating the secretion of Timp1 on DC cells.

On the basis of these data and of the existing literature, we raised a working hypothesis which could explain the MPE formation: Tumor cells secrete CCL2 to attract mononuclear cells into the pleural cavity which further mature into macrophages. These Macrophages also produce CCL2, which further induce more influx of inflammatory monocytes to the pleural cavity. Meanwhile, through Axl and Mertk receptors, macrophages sense the apoptotic cells in MPE environment and by producing IL-10 promote the expression of Timp1 in DCs. Timp1 affects the extracellular matrix components of the pleura, which increases the vascular permeability, favoring the influx of the fluid into the pleural cavity and therefore the development of MPE.

4. Discussion

Malignant pleural effusion (MPE) is a common complication of advanced malignant tumors, of which lung cancer and breast cancer are the most common (Villena Garrido et al., 2014). Evidence from mouse models and humans indicates that the complex inflammatory interactions, including tumor cells and the host's vascular and immune systems, lead to sharp elevations of inflammatory and vasoactive mediator levels in the pleural fluid, renders pleural blood vessels leaky and directly leads to MPE formation (Stathopoulos and Kalomenidis, 2012). We identified that, macrophages sensed the apoptotic cells through Axl and Mertk receptors, and then produced IL-10, which promoted MPE by activating the secretion of Timp1 on dendritic cells.

IL-10 is often referred to as a pleiotropic cytokine, and its dual role in cancer likely reflects this. Both IL-10-deficiency and IL-10-overexpression can promote anti-tumor immune responses in mice (O'Garra et al., 2008). While IL-10-deficient mice are resistant to ultraviolet-induced skin carcinogenesis (Loser et al., 2007), they are also sensitive to skin and colon carcinogenesis (Mumm et al., 2011; Sturlan et al., 2001). Such disparity mostly reflects the significance of local tumor microenvironments in sculpting immune responses, but also likely reflects local functional activity of IL-10 (O'Garra et al., 2008). Some studies showed that the concentration of IL-10 in MPE was higher than in peripheral blood (Chen et al., 1996; Klimatsidas et al., 2012), while other researchers reported IL-10 level was not significantly different between MPE and peripheral blood (Li et al., 2016). In our study, we further check the IL-10 level in both MPE and benign pleural effusion (BPE) from humans, and we found that the concentration of IL-10 is higher in MPE, which indicates that IL-10 could be more important in inflammatory (exudative) effusions than in transudate effusions. Interestingly, the

fact that BPE contained also IL-10, although in less amounts, suggests that its source is not only from tumor cells but also from other cells, such as macrophages or pleural mesothelial cells. Both cell types have been shown to produce these cytokine (Chen et al., 1996; Cheng et al., 2000; Sikora et al., 2004). In parallel, we further used a loss-of-function method and found that IL-10 could promote MPE formation, and the median survival time of MPE-bearing IL-10 deficient mice was longer than MPE-bearing wildtype mice, while IL-10 doesn't have impact on tumor growth. Consistently, Wu *et al.* (Wu et al., 2019) also showed that IL-10 promotes MPE in mice, and they claim that it is due to the function of IL-10 by regulating Th1- and Th17-cell differentiation and migration. Taken together, these findings suggested that IL-10 is a pro-MPE cytokine.

It has been well documented that various leukocyte populations (Saraiva and O'Garra, 2010), as well as normal and malignant epithelial cells (O'Garra et al., 2008) could express IL-10. In this study, we used IL-10^{eGFP} tiger mice, 10Bit reporter mice as well as C57BL/6 mice to identify the cellular source of IL-10 in MPE, which turns out to be myeloid cells, especially macrophages. Multiple studies have found a positive correlation between IL-10 levels (both in serum and within the tumor) and poor prognosis for the various forms of cancer patients, including lung cancer (Li et al., 2014), melanoma (Boyano et al., 2000; Sato et al., 1996), and lymphomas (Boulland et al., 1998). IL-10, by reducing or inhibiting antigen presentation via downregulation of MHC class II expression (Steinbrink et al., 1999) in APCs as well as MHC class I in tumor cells (Adris et al., 1999), contribute to an immunosuppressive environment and thus facilitate tumor escape. As previously stated, certain types of macrophages, notably, M2-macrophages, have been shown to release significant amounts of IL-10 in the tumor microenvironment (Wang et al., 2012), suggesting a correlation between IL-10 and tumor development. We also identify IL-10 producing macrophages in

MPE, which is consistent with the findings that the tumor microenvironment may contain many IL-10 producing macrophages.

It has been recognized that depletion of circulating monocytes/macrophages (e.g., using *Ccr2*^{-/-} mice or *via* the systemic administration of liposomal clodronate) ameliorates MPE formation (Giannou et al., 2015). Reducing the number of macrophages in breast cancer slowed pre-invasive change to full tumor, with simultaneous reduction of the formation of lung metastases (Lin et al., 2001). Elimination of macrophages also decreased the density of vascularity in advanced cancer by 50% (Lewis and Murdoch, 2005). Our data showed that part of the macrophages produce IL-10, suggesting macrophages are a heterogeneous population, instead of depleting all macrophages which might include potential “con-MPE” one, targeting only the specific pro-MPE macrophages would inhibit them from being more efficient for impairing MPE development.

Single cell RNA sequencing (scRNA-seq) uniquely enabled us to quantify differences between subpopulations of the macrophages. Till now such an approach has not been performed in MPE. Using scRNA-seq, we investigated in an unbiased manner, the myeloid cells infiltrate in pleural cavity and uncovered here 4 major macrophage populations. We then revealed their gene expression signature. The 4 identified macrophage populations displayed a common bona fide macrophage gene signature (e.g. *Itgam*) and a promigratory profile. All these four populations are indeed characterized by the expression of *Ccl2* which transcribed for a key chemokine to recruit more monocytes. This could initiate a pro-inflammatory loop by propagating and amplifying the inflammatory cascade (Mantovani et al., 2008). Functional enrichment analysis revealed critical functions of macrophages in MPE development, such as angiogenesis (eg. *Ccl2*,

Arg1 and *Hif1a*), tissue remodeling (eg. *Retnla*, *Chil3*, *Ear2* and *Fn1*) and cell migration (eg. *Pf4*, *Ccl7*, *Trem2* and *Pppb*). Traditionally, macrophages in MPE are predominantly so-called M2-polarized and BPE are predominantly M1-polarized (Kaczmarek et al., 2018). Studies have also shown that the frequency of CD163+ (M2 marker) macrophages in MPE are significantly higher than that in BPE (Wang et al., 2015). In line with the literatures, the gene expression profile of cells of cluster 0 and cluster 1 was reminiscent of M2 macrophages with expression of *Mrc1* and *Arg1* and low expression of proinflammatory cytokines, such as *Tnf* or *Il1b*, suggesting a pro-MPE phenotype. Moreover, *Il10* is highly expressed in cells of cluster 0 and 1. However, the other two populations of macrophages (cluster 2 and cluster 3) did not display any gene expression patterns linking them to previously proposed M2 macrophage subtypes. These findings clarify that applying the rigid, simplified nomenclature previously defined cannot explain the MPE macrophage heterogeneity.

What promotes the IL-10 expression in MPE macrophages is unclear. In general, IL-10 expression by macrophages is thought to be induced by TLR ligands and type I IFN (Saraiva and O'Garra, 2010). However, increasing evidence demonstrates that by phagocytosing the apoptotic cells through TAM receptor tyrosine kinases (TYRO3, AXL, and MERTK), macrophages could produce IL-10 (Bosurgi et al., 2013). This is the first study which focused on the role of TAM receptors in MPE. Our results support the notion that the TAM receptors are involved in efferocytosis of apoptosis cells generated during MPE development. An important feature of macrophages ingesting apoptosis cells is their subsequent propensity to downregulate the generation of proinflammatory cytokines and upregulate factors associated with immunosuppression (Fadok et al., 1998a; Fadok et al., 1998b; Filardy et al., 2010). In a model of DSS-induced colitis, macrophages from *Axl*^{-/-}*Mertk*^{-/-} mice showed markedly impaired

production of tissue repair factors including Relm- α , TGF- β , and IL-10 (Bosurgi et al., 2013). A number of small molecule inhibitors targeting the TAM receptors for cancer therapy are in development (Hector et al., 2010; Holland et al., 2010; Rettew et al., 2012). The TAM receptors might be ideal targets for pharmacological intervention and disabling their function will likely prove efficacious in MPE patients.

We further investigated the target cells of IL-10 in MPE. We identified that CD45⁺ leukocyte express the Il10ra, and *in vitro* experiment further show that CD3⁻ cells are able to respond to IL-10 stimulation. Furthermore, scRNA-seq results indicated that dendritic cells (DCs) might be the target cells of IL-10 since DCs showed the highest Il10ra expression. DCs are professional antigen presenting cells (APCs) that present antigens, induce adaptive immune responses, and regulate the immune system by modulating T and B lymphocyte antigen specific responses via their major histocompatibility (MHC) class I and II receptors (Mellman, 2013). A meta-analysis evaluating the significance of immune cells in NSCLC showed that increased tumor and stromal conventional dendritic cells (cDCs) were associated with improved survival (Soo et al., 2018). DCs isolated from lung cancer MPE patients expressed higher levels of CD86, HLA-DR, CD40, CD1a, and but lower CD14 compared to DCs from benign effusions (Zhong et al., 2004). Previous reports indicated that DCs from MPE showed HLA-DR⁺ immunosuppressive phenotype (Gjomarkaj et al., 1997). For example, DCs were reported to expand Tregs and suppress CD8 T cells to establish an immunosuppressive microenvironment leading to metastasis formation in pancreatic cancer (Kenkel et al., 2017). These results suggest that DCs are present in exudative pleural effusions, and they may be involved in the development of cell-mediated immune reactions in the pleural space.

In this study, we identified that DCs expressed Timp1 (tissue inhibitor of metalloproteinases 1), which bind irreversibly to matrix metalloproteinases (MMPs) and inhibit their action. MMPs is a large family, which is named for its need for metal ions such as Ca^{2+} and Zn^{2+} as cofactors. They are proteolytic enzymes that hydrolyzes the extracellular matrix (ECM), including various collagenases and elastases. The deregulation of the expression balance of TIMPs and MMPs happens in the tumor microenvironment, which could degrade various protein components in ECM, destroy the histological barrier, and promote tumor invasion and metastasis. Our results indicated that Timp1 is abundant in both human and mice lung tissue, suggesting its tissue remodeling function. In addition, exposure to IL-10 could promote Timp1 production by DCs, indicating a possible role of DCs in tissue remodelling, as well as in MPE development. Psallidas *et al.* (Psallidas et al., 2018) found that pleural fluid TIMP1 concentrations are associated with survival in MPE patients. Previous studies also suggested that TIMP1 promotes cellular proliferation and anti-apoptotic activity (Guedez et al., 1998; Kim et al., 2012; Luparello et al., 1999). Hence, Timp1 could be a potential target in controlling MPE development, and further work is required to elucidate mechanisms of Timp1 function within MPE.

In this study, we used a mouse model to study the role and the related mechanisms of macrophages in the occurrence and development of MPE. We demonstrated that macrophages derived IL-10 could promote MPE formation and accelerate the death of the mice. The scRNA-seq helped us to understand the phenotype and functional characteristics of macrophages in MPE, such as the key genes as well as their impact on MPE progression and outcome. Of note, this study is the first one that systematically characterizes the myeloid cells of pleural fluid. Given the heterogeneity observed in the myeloid cells in MPE, a larger prospective validation clinical study will also clarify if the inter-patients and

intra-patients variability could also be observed in human MPE, and to identify potential prognostic factors. This may contribute to a more accurate patients' stratification, for a rationale and personalized immune-therapy of MPE. Our study also reveals new mechanisms of immune cell and cytokine networks (including macrophages, IL-10 and DCs as key players in the pleural space) during MPE. Since IL-10 could induce DCs to produce Timp1, and the blockade of IL-10 as well as the Timp1 may be novel approaches to prevent or alleviate MPE in patients with cancer. As highlighted above, advances in our understanding of tumor immunology in conjunction with technological innovations will yield novel immune-based treatments and will result in unprecedented clinical success for MPE treatment.

5. Summary

MPE is a sign in advanced cancer patients, especially lung cancer, patients develop fluid in their pleural space and lead to compressed lung tissue. MPE is associated with significant mortality and current therapies are inefficient. Our results from mouse models and humans suggests that the immune system is playing a key role in MPE formation. Immune cells are attracted by tumors and secrete chemokines and cytokines, to promote angiogenesis, vascular leakage leading to higher amount of fluid in the pleural space. Using intrapleural injection models of lung metastasis in mice, we found that IL-10 is abundant in the microenvironment of the pleural cavity. Genetic IL-10 deficiency offered marked protection of the mice from pleural effusion formation of different types of tumor cells, including lung cancer and colon cancer. However, IL-10 deficiency did not affect the growth of the size of metastatic lesions. Mechanistic investigations revealed that macrophages sense and phagocyte the apoptotic cells through Axl and Mertk receptors and produce IL-10. IL-10 created a proangiogenic, high vascular permeability microenvironment, potentially by inducing dendritic cells-derived Timp1 expression. Together, our results establish a network of inflammatory cascade that can be co-opted by metastatic cancer cells to facilitate pleural effusion formation, suggesting interventions to target this pathway may offer therapeutic benefits to prevent or treat MPE.

Zusammenfassung

Maligner Pleuraerguss (MPE) ist ein Zeichen für fortgeschrittene Krebspatienten, insbesondere für Lungenkrebspatienten. Patienten entwickeln Flüssigkeit in ihrem Pleuraraum und dies führt zu komprimiertem Lungengewebe. MPE ist mit einer signifikanten Mortalität verbunden und die derzeitigen Therapien sind ineffizient. Unsere Ergebnisse aus Mausmodellen und Menschen legen nahe, dass das Immunsystem eine Schlüsselrolle bei der Bildung von MPE spielt. Immunzellen werden von Tumoren angezogen und scheiden Chemokine und Zytokine aus, um die Angiogenese zu fördern. Gefäßleckagen führen zu einer höheren Flüssigkeitsmenge im Pleuraraum. Unter Verwendung von intrapleuralem Injektionsmodellen der Lungenmetastasierung bei Mäusen fanden wir, dass IL-10 in der Mikroumgebung der Pleurahöhle häufig vorkommt. Der genetische IL-10-Mangel bot den Mäusen einen deutlichen Schutz vor der Bildung von Pleuraergüssen verschiedener Arten von Tumorzellen, einschließlich Lungenkrebs und Dickdarmkrebs. Ein IL-10-Mangel hatte jedoch keinen Einfluss auf das Wachstum der Größe metastatischer Läsionen. Mechanistische Untersuchungen ergaben, dass Makrophagen die apoptotischen Zellen über Axl- und Mertk-Rezeptoren wahrnehmen und phagozytieren und IL-10 produzieren. IL-10 erzeugte eine proangiogene Mikroumgebung mit hoher Gefäßpermeabilität, möglicherweise durch Induktion der von dendritischen Zellen abgeleiteten Timp1-Expression. Zusammengefasst etablieren unsere Ergebnisse ein Netzwerk von Entzündungskaskaden, die von metastasierenden Krebszellen kooptiert werden können, um die Bildung von Pleuraergüssen zu erleichtern. Dies lässt darauf schließen, dass Interventionen, die auf diesen Weg abzielen, therapeutische Vorteile zur Vorbeugung oder Behandlung von MPE bieten können.

6. Reference

Adris, S., Klein, S., Jasnis, M., Chuluyan, E., Ledda, M., Bravo, A., Carbone, C., Chernajovsky, Y., Podhajcer, O., 1999. IL-10 expression by CT26 colon carcinoma cells inhibits their malignant phenotype and induces a T cell-mediated tumor rejection in the context of a systemic Th2 response. *Gene Ther* 6, 1705-1712.

Agalioti, T., Giannou, A.D., Krontira, A.C., Kanellakis, N.I., Kati, D., Vreka, M., Pepe, M., Spella, M., Lilis, I., Zazara, D.E., Nikolouli, E., Spiropoulou, N., Papadakis, A., Papadia, K., Voulgaridis, A., Harokopos, V., Stamou, P., Meiners, S., Eickelberg, O., Snyder, L.A., Antimisiaris, S.G., Kardamakis, D., Psallidas, I., Marazioti, A., Stathopoulos, G.T., 2017. Mutant KRAS promotes malignant pleural effusion formation. *Nat Commun* 8, 15205.

Akalu, Y.T., Rothlin, C.V., Ghosh, S., 2017. TAM receptor tyrosine kinases as emerging targets of innate immune checkpoint blockade for cancer therapy. *Immunol Rev* 276, 165-177.

Amir el, A.D., Davis, K.L., Tadmor, M.D., Simonds, E.F., Levine, J.H., Bendall, S.C., Shenfeld, D.K., Krishnaswamy, S., Nolan, G.P., Pe'er, D., 2013. viSNE enables visualization of high dimensional single-cell data and reveals phenotypic heterogeneity of leukemia. *Nat Biotechnol* 31, 545-552.

Arango Duque, G., Descoteaux, A., 2014. Macrophage cytokines: involvement in immunity and infectious diseases. *Front Immunol* 5, 491.

Bosurgi, L., Bernink, J.H., Delgado Cuevas, V., Gagliani, N., Joannas, L., Schmid, E.T., Booth, C.J., Ghosh, S., Rothlin, C.V., 2013. Paradoxical role of the proto-oncogene Axl and Mer receptor tyrosine kinases in colon cancer. *Proc Natl Acad Sci U S A* 110, 13091-13096.

Boulland, M.L., Meignin, V., Leroy-Viard, K., Copie-Bergman, C., Briere, J., Toutou, R., Kanavaros, P., Gaulard, P., 1998. Human interleukin-10 expression in T/natural killer-cell lymphomas: association with anaplastic large cell lymphomas and nasal natural killer-cell lymphomas. *Am J Pathol* 153, 1229-1237.

Bourreille, A., Segain, J.P., Raingeard de la Bletiere, D., Siavoshian, S., Vallette, G., Galmiche, J.P., Blottiere, H.M., 1999. Lack of interleukin 10 regulation of antigen presentation-associated molecules expressed on colonic epithelial cells. *Eur J Clin Invest* 29, 48-55.

Boyano, M.D., Garcia-Vazquez, M.D., Lopez-Michelena, T., Gardeazabal, J., Bilbao, J., Canavate, M.L., Galdeano, A.G., Izu, R., Diaz-Ramon, L., Raton, J.A., Diaz-Perez, J.L., 2000. Soluble interleukin-2 receptor, intercellular adhesion

molecule-1 and interleukin-10 serum levels in patients with melanoma. *Br J Cancer* 83, 847-852.

Chang, Y.H., Chiu, Y.J., Cheng, H.C., Liu, F.J., Lai, W.W., Chang, H.J., Liao, P.C., 2015. Down-regulation of TIMP-1 inhibits cell migration, invasion, and metastatic colonization in lung adenocarcinoma. *Tumour Biol* 36, 3957-3967.

Chen, Y.M., Yang, W.K., Whang-Peng, J., Kuo, B.I., Perng, R.P., 1996. Elevation of interleukin-10 levels in malignant pleural effusion. *Chest* 110, 433-436.

Chen, Y.Q., Shi, H.Z., Qin, X.J., Mo, W.N., Liang, X.D., Huang, Z.X., Yang, H.B., Wu, C., 2005. CD4+CD25+ regulatory T lymphocytes in malignant pleural effusion. *Am J Respir Crit Care Med* 172, 1434-1439.

Cheng, D., Lee, Y.C., Rogers, J.T., Perkett, E.A., Moyers, J.P., Rodriguez, R.M., Light, R.W., 2000. Vascular endothelial growth factor level correlates with transforming growth factor-beta isoform levels in pleural effusions. *Chest* 118, 1747-1753.

Cheng, F., Torzewski, M., Degreif, A., Rossmann, H., Canisius, A., Lackner, K.J., 2013. Impact of glutathione peroxidase-1 deficiency on macrophage foam cell formation and proliferation: implications for atherogenesis. *PLoS One* 8, e72063.

Chung, E.Y., Liu, J., Homma, Y., Zhang, Y., Brendolan, A., Saggese, M., Han, J., Silverstein, R., Selleri, L., Ma, X., 2007. Interleukin-10 expression in macrophages during phagocytosis of apoptotic cells is mediated by homeodomain proteins Pbx1 and Prep-1. *Immunity* 27, 952-964.

Clive, A.O., Kahan, B.C., Hooper, C.E., Bhatnagar, R., Morley, A.J., Zahan-Evans, N., Bintcliffe, O.J., Boshuizen, R.C., Fysh, E.T., Tobin, C.L., Medford, A.R., Harvey, J.E., van den Heuvel, M.M., Lee, Y.C., Maskell, N.A., 2014. Predicting survival in malignant pleural effusion: development and validation of the LENT prognostic score. *Thorax* 69, 1098-1104.

Consortium, G.T., 2013. The Genotype-Tissue Expression (GTEx) project. *Nat Genet* 45, 580-585.

Cook, R.S., Jacobsen, K.M., Wofford, A.M., DeRyckere, D., Stanford, J., Prieto, A.L., Redente, E., Sandahl, M., Hunter, D.M., Strunk, K.E., Graham, D.K., Earp, H.S., 3rd, 2013. MerTK inhibition in tumor leukocytes decreases tumor growth and metastasis. *J Clin Invest* 123, 3231-3242.

Crepaldi, L., Gasperini, S., Lapinet, J.A., Calzetti, F., Pinardi, C., Liu, Y., Zurawski, S., de Waal Malefyt, R., Moore, K.W., Cassatella, M.A., 2001. Up-

regulation of IL-10R1 expression is required to render human neutrophils fully responsive to IL-10. *J Immunol* 167, 2312-2322.

Cui, H., Seubert, B., Stahl, E., Dietz, H., Reuning, U., Moreno-Leon, L., Ilie, M., Hofman, P., Nagase, H., Mari, B., Kruger, A., 2015. Tissue inhibitor of metalloproteinases-1 induces a pro-tumourigenic increase of miR-210 in lung adenocarcinoma cells and their exosomes. *Oncogene* 34, 3640-3650.

Denning, T.L., Campbell, N.A., Song, F., Garofalo, R.P., Klimpel, G.R., Reyes, V.E., Ernst, P.B., 2000. Expression of IL-10 receptors on epithelial cells from the murine small and large intestine. *Int Immunol* 12, 133-139.

Ellis, L.M., Liu, W., Ahmad, S.A., Fan, F., Jung, Y.D., Shaheen, R.M., Reinmuth, N., 2001. Overview of angiogenesis: Biologic implications for antiangiogenic therapy. *Semin Oncol* 28, 94-104.

Fadok, V.A., Bratton, D.L., Konowal, A., Freed, P.W., Westcott, J.Y., Henson, P.M., 1998a. Macrophages that have ingested apoptotic cells in vitro inhibit proinflammatory cytokine production through autocrine/paracrine mechanisms involving TGF-beta, PGE2, and PAF. *J Clin Invest* 101, 890-898.

Fadok, V.A., McDonald, P.P., Bratton, D.L., Henson, P.M., 1998b. Regulation of macrophage cytokine production by phagocytosis of apoptotic and post-apoptotic cells. *Biochem Soc Trans* 26, 653-656.

Fadok, V.A., Voelker, D.R., Campbell, P.A., Cohen, J.J., Bratton, D.L., Henson, P.M., 1992. Exposure of phosphatidylserine on the surface of apoptotic lymphocytes triggers specific recognition and removal by macrophages. *J Immunol* 148, 2207-2216.

Fang, F., Chen, P., Wu, X., Yang, L., Yang, X., Xi, Z.X., Zhou, B.W., Zhou, X.K., Qian, Z.Y., Xiao, B., Wei, Y.Q., 2009. Therapeutic effects of recombinant human endostatin adenovirus in a mouse model of malignant pleural effusion. *J Cancer Res Clin Oncol* 135, 1149-1157.

Faul, F., Erdfelder, E., Lang, A.G., Buchner, A., 2007. G*Power 3: a flexible statistical power analysis program for the social, behavioral, and biomedical sciences. *Behav Res Methods* 39, 175-191.

Feller-Kopman, D., Light, R., 2018. Pleural Disease. *N Engl J Med* 378, 740-751.

Filardy, A.A., Pires, D.R., Nunes, M.P., Takiya, C.M., Freire-de-Lima, C.G., Ribeiro-Gomes, F.L., DosReis, G.A., 2010. Proinflammatory clearance of apoptotic neutrophils induces an IL-12(low)IL-10(high) regulatory phenotype in macrophages. *J Immunol* 185, 2044-2050.

Finbloom, D.S., Winestock, K.D., 1995. IL-10 induces the tyrosine phosphorylation of tyk2 and Jak1 and the differential assembly of STAT1 alpha and STAT3 complexes in human T cells and monocytes. *J Immunol* 155, 1079-1090.

Fiorentino, D.F., Bond, M.W., Mosmann, T.R., 1989. Two types of mouse T helper cell. IV. Th2 clones secrete a factor that inhibits cytokine production by Th1 clones. *J Exp Med* 170, 2081-2095.

Gabrysova, L., Howes, A., Saraiva, M., O'Garra, A., 2014. The regulation of IL-10 expression. *Curr Top Microbiol Immunol* 380, 157-190.

Gautier, E.L., Shay, T., Miller, J., Greter, M., Jakubzick, C., Ivanov, S., Helft, J., Chow, A., Elpek, K.G., Gordonov, S., Mazloom, A.R., Ma'ayan, A., Chua, W.J., Hansen, T.H., Turley, S.J., Merad, M., Randolph, G.J., Immunological Genome, C., 2012. Gene-expression profiles and transcriptional regulatory pathways that underlie the identity and diversity of mouse tissue macrophages. *Nat Immunol* 13, 1118-1128.

Giannou, A.D., Marazioti, A., Spella, M., Kanellakis, N.I., Apostolopoulou, H., Psallidas, I., Prijovich, Z.M., Vreka, M., Zazara, D.E., Lilis, I., Papaleonidopoulos, V., Kairi, C.A., Patmanidi, A.L., Giopanou, I., Spiropoulou, N., Harokopos, V., Aidinis, V., Spyrtos, D., Teliousi, S., Papadaki, H., Taraviras, S., Snyder, L.A., Eickelberg, O., Kardamakis, D., Iwakura, Y., Feyerabend, T.B., Rodewald, H.R., Kalomenidis, I., Blackwell, T.S., Agalioti, T., Stathopoulos, G.T., 2015. Mast cells mediate malignant pleural effusion formation. *J Clin Invest* 125, 2317-2334.

Gibbs, V.C., Pennica, D., 1997. CRF2-4: isolation of cDNA clones encoding the human and mouse proteins. *Gene* 186, 97-101.

Giri, J.G., Wells, J., Dower, S.K., McCall, C.E., Guzman, R.N., Slack, J., Bird, T.A., Shanebeck, K., Grabstein, K.H., Sims, J.E., et al., 1994. Elevated levels of shed type II IL-1 receptor in sepsis. Potential role for type II receptor in regulation of IL-1 responses. *J Immunol* 153, 5802-5809.

Gjomarkaj, M., Pace, E., Melis, M., Spatafora, M., D'Amico, D., Toews, G.B., 1997. Dendritic cells with a potent accessory activity are present in human exudative malignant pleural effusions. *Eur Respir J* 10, 592-597.

Gordon, S., Martinez, F.O., 2010. Alternative activation of macrophages: mechanism and functions. *Immunity* 32, 593-604.

Guedez, L., Stetler-Stevenson, W.G., Wolff, L., Wang, J., Fukushima, P., Mansoor, A., Stetler-Stevenson, M., 1998. In vitro suppression of programmed

cell death of B cells by tissue inhibitor of metalloproteinases-1. *J Clin Invest* 102, 2002-2010.

Hashimoto, D., Chow, A., Noizat, C., Teo, P., Beasley, M.B., Leboeuf, M., Becker, C.D., See, P., Price, J., Lucas, D., Greter, M., Mortha, A., Boyer, S.W., Forsberg, E.C., Tanaka, M., van Rooijen, N., Garcia-Sastre, A., Stanley, E.R., Ginhoux, F., Frenette, P.S., Merad, M., 2013. Tissue-resident macrophages self-maintain locally throughout adult life with minimal contribution from circulating monocytes. *Immunity* 38, 792-804.

Hector, A., Montgomery, E.A., Karikari, C., Canto, M., Dunbar, K.B., Wang, J.S., Feldmann, G., Hong, S.M., Haffner, M.C., Meeker, A.K., Holland, S.J., Yu, J., Heckrodt, T.J., Zhang, J., Ding, P., Goff, D., Singh, R., Roa, J.C., Marimuthu, A., Riggins, G.J., Eshleman, J.R., Nelkin, B.D., Pandey, A., Maitra, A., 2010. The Axl receptor tyrosine kinase is an adverse prognostic factor and a therapeutic target in esophageal adenocarcinoma. *Cancer Biol Ther* 10, 1009-1018.

Heffner, J.E., Brown, L.K., Barbieri, C.A., 1997. Diagnostic value of tests that discriminate between exudative and transudative pleural effusions. *Primary Study Investigators. Chest* 111, 970-980.

Heinrich, P.C., Behrmann, I., Muller-Newen, G., Schaper, F., Graeve, L., 1998. Interleukin-6-type cytokine signalling through the gp130/Jak/STAT pathway. *Biochem J* 334 (Pt 2), 297-314.

Holland, S.J., Pan, A., Franci, C., Hu, Y., Chang, B., Li, W., Duan, M., Torneros, A., Yu, J., Heckrodt, T.J., Zhang, J., Ding, P., Apatira, A., Chua, J., Brandt, R., Pine, P., Goff, D., Singh, R., Payan, D.G., Hitoshi, Y., 2010. R428, a selective small molecule inhibitor of Axl kinase, blocks tumor spread and prolongs survival in models of metastatic breast cancer. *Cancer Res* 70, 1544-1554.

Huang, M., Sharma, S., Mao, J.T., Dubinett, S.M., 1996. Non-small cell lung cancer-derived soluble mediators and prostaglandin E2 enhance peripheral blood lymphocyte IL-10 transcription and protein production. *J Immunol* 157, 5512-5520.

Huber, S., Gagliani, N., Esplugues, E., O'Connor, W., Jr., Huber, F.J., Chaudhry, A., Kamanaka, M., Kobayashi, Y., Booth, C.J., Rudensky, A.Y., Roncarolo, M.G., Battaglia, M., Flavell, R.A., 2011. Th17 cells express interleukin-10 receptor and are controlled by Foxp3(-) and Foxp3+ regulatory CD4+ T cells in an interleukin-10-dependent manner. *Immunity* 34, 554-565.

Janssen, W.J., Barthel, L., Muldrow, A., Oberley-Deegan, R.E., Kearns, M.T., Jakubzick, C., Henson, P.M., 2011. Fas determines differential fates of resident

and recruited macrophages during resolution of acute lung injury. *Am J Respir Crit Care Med* 184, 547-560.

Jou, I.M., Lin, C.F., Tsai, K.J., Wei, S.J., 2013. Macrophage-mediated inflammatory disorders. *Mediators Inflamm* 2013, 316482.

Kaczmarek, M., Lagiedo, M., Masztalerz, A., Kozłowska, M., Nowicka, A., Brajer, B., Batura-Gabryel, H., Sikora, J., 2018. Concentrations of SP-A and HSP70 are associated with polarization of macrophages in pleural effusions of non-small cell lung cancer. *Immunobiology* 223, 200-209.

Kaczmarek, M., Sikora, J., 2012. Macrophages in malignant pleural effusions - alternatively activated tumor associated macrophages. *Contemp Oncol (Pozn)* 16, 279-284.

Kamanaka, M., Huber, S., Zenewicz, L.A., Gagliani, N., Rathinam, C., O'Connor, W., Jr., Wan, Y.Y., Nakae, S., Iwakura, Y., Hao, L., Flavell, R.A., 2011. Memory/effector (CD45RB(lo)) CD4 T cells are controlled directly by IL-10 and cause IL-22-dependent intestinal pathology. *J Exp Med* 208, 1027-1040.

Kamanaka, M., Kim, S.T., Wan, Y.Y., Sutterwala, F.S., Lara-Tejero, M., Galan, J.E., Harhaj, E., Flavell, R.A., 2006. Expression of interleukin-10 in intestinal lymphocytes detected by an interleukin-10 reporter knockin tiger mouse. *Immunity* 25, 941-952.

Karmaus, P.W.F., Herrada, A.A., Guy, C., Neale, G., Dhungana, Y., Long, L., Vogel, P., Avila, J., Clish, C.B., Chi, H., 2017. Critical roles of mTORC1 signaling and metabolic reprogramming for M-CSF-mediated myelopoiesis. *J Exp Med* 214, 2629-2647.

Kenkel, J.A., Tseng, W.W., Davidson, M.G., Tolentino, L.L., Choi, O., Bhattacharya, N., Seeley, E.S., Winer, D.A., Reticker-Flynn, N.E., Engleman, E.G., 2017. An Immunosuppressive Dendritic Cell Subset Accumulates at Secondary Sites and Promotes Metastasis in Pancreatic Cancer. *Cancer Res* 77, 4158-4170.

Kim, Y.S., Kim, S.H., Kang, J.G., Ko, J.H., 2012. Expression level and glycan dynamics determine the net effects of TIMP-1 on cancer progression. *BMB Rep* 45, 623-628.

Klimatsidas, M., Anastasiadis, K., Foroulis, C., Tossios, P., Bisiklis, A., Papakonstantinou, C., Rammos, K., 2012. Elevated levels of anti inflammatory IL-10 and pro inflammatory IL-17 in malignant pleural effusions. *J Cardiothorac Surg* 7, 104.

- Kohno, T., Mizukami, H., Suzuki, M., Saga, Y., Takei, Y., Shimpo, M., Matsushita, T., Okada, T., Hanazono, Y., Kume, A., Sato, I., Ozawa, K., 2003. Interleukin-10-mediated inhibition of angiogenesis and tumor growth in mice bearing VEGF-producing ovarian cancer. *Cancer Res* 63, 5091-5094.
- Kotenko, S.V., Krause, C.D., Izotova, L.S., Pollack, B.P., Wu, W., Pestka, S., 1997. Identification and functional characterization of a second chain of the interleukin-10 receptor complex. *EMBO J* 16, 5894-5903.
- Kovach, M.A., Stringer, K.A., Bunting, R., Wu, X., San Mateo, L., Newstead, M.W., Paine, R., Standiford, T.J., 2015. Microarray analysis identifies IL-1 receptor type 2 as a novel candidate biomarker in patients with acute respiratory distress syndrome. *Respir Res* 16, 29.
- Kuhn, R., Lohler, J., Rennick, D., Rajewsky, K., Muller, W., 1993. Interleukin-10-deficient mice develop chronic enterocolitis. *Cell* 75, 263-274.
- Lewis, C., Murdoch, C., 2005. Macrophage responses to hypoxia: implications for tumor progression and anti-cancer therapies. *Am J Pathol* 167, 627-635.
- Li, C., Li, H., Jiang, K., Li, J., Gai, X., 2014. TLR4 signaling pathway in mouse Lewis lung cancer cells promotes the expression of TGF-beta1 and IL-10 and tumor cells migration. *Biomed Mater Eng* 24, 869-875.
- Li, C., Zhao, B., Lin, C., Gong, Z., An, X., 2019. TREM2 inhibits inflammatory responses in mouse microglia by suppressing the PI3K/NF-kappaB signaling. *Cell Biol Int* 43, 360-372.
- Li, L., Yang, L., Wang, L., Wang, F., Zhang, Z., Li, J., Yue, D., Chen, X., Ping, Y., Huang, L., Zhang, B., Zhang, Y., 2016. Impaired T cell function in malignant pleural effusion is caused by TGF-beta derived predominantly from macrophages. *Int J Cancer* 139, 2261-2269.
- Light, R.W., 2013. *Pleural Diseases*, 6 ed. Lippincott Williams & Wilkins, Philadelphia.
- Light, R.W., Macgregor, M.I., Luchsinger, P.C., Ball, W.C., Jr., 1972. Pleural effusions: the diagnostic separation of transudates and exudates. *Ann Intern Med* 77, 507-513.
- Lim, J.P., Teasdale, R.D., Gleeson, P.A., 2012. SNX5 is essential for efficient macropinocytosis and antigen processing in primary macrophages. *Biol Open* 1, 904-914.

- Lin, E.Y., Nguyen, A.V., Russell, R.G., Pollard, J.W., 2001. Colony-stimulating factor 1 promotes progression of mammary tumors to malignancy. *J Exp Med* 193, 727-740.
- Lin, H., Tong, Z.H., Xu, Q.Q., Wu, X.Z., Wang, X.J., Jin, X.G., Ma, W.L., Cheng, X., Zhou, Q., Shi, H.Z., 2014. Interplay of Th1 and Th17 cells in murine models of malignant pleural effusion. *Am J Respir Crit Care Med* 189, 697-706.
- Lishko, V.K., Yakubenko, V.P., Ugarova, T.P., Podolnikova, N.P., 2018. Leukocyte integrin Mac-1 (CD11b/CD18, alphaMbeta2, CR3) acts as a functional receptor for platelet factor 4. *J Biol Chem* 293, 6869-6882.
- Loser, K., Apelt, J., Voskort, M., Mohaupt, M., Balkow, S., Schwarz, T., Grabbe, S., Beissert, S., 2007. IL-10 controls ultraviolet-induced carcinogenesis in mice. *J Immunol* 179, 365-371.
- Lucivero, G., Pierucci, G., Bonomo, L., 1988. Lymphocyte subsets in peripheral blood and pleural fluid. *Eur Respir J* 1, 337-340.
- Luparello, C., Avanzato, G., Carella, C., Pucci-Minafra, I., 1999. Tissue inhibitor of metalloprotease (TIMP)-1 and proliferative behaviour of clonal breast cancer cells. *Breast Cancer Res Treat* 54, 235-244.
- Lutfalla, G., Gardiner, K., Uze, G., 1993. A new member of the cytokine receptor gene family maps on chromosome 21 at less than 35 kb from IFNAR. *Genomics* 16, 366-373.
- Lv, M., Xu, Y., Tang, R., Ren, J., Shen, S., Chen, Y., Liu, B., Hou, Y., Wang, T., 2014. miR141-CXCL1-CXCR2 signaling-induced Treg recruitment regulates metastases and survival of non-small cell lung cancer. *Mol Cancer Ther* 13, 3152-3162.
- Ma, X., Yao, Y., Yuan, D., Liu, H., Wang, S., Zhou, C., Song, Y., 2012. Recombinant human endostatin endostar suppresses angiogenesis and lymphangiogenesis of malignant pleural effusion in mice. *PLoS One* 7, e53449.
- Mantovani, A., Allavena, P., Sica, A., Balkwill, F., 2008. Cancer-related inflammation. *Nature* 454, 436-444.
- Marazioti, A., Kairi, C.A., Spella, M., Giannou, A.D., Magkouta, S., Giopanou, I., Papaleonidopoulos, V., Kalomenidis, I., Snyder, L.A., Kardamakis, D., Stathopoulos, G.T., 2013. Beneficial impact of CCL2 and CCL12 neutralization on experimental malignant pleural effusion. *PLoS One* 8, e71207.

Martin, P., Palmer, G., Vigne, S., Lamacchia, C., Rodriguez, E., Talabot-Ayer, D., Rose-John, S., Chalaris, A., Gabay, C., 2013. Mouse neutrophils express the decoy type 2 interleukin-1 receptor (IL-1R2) constitutively and in acute inflammatory conditions. *J Leukoc Biol* 94, 791-802.

Mauer, J., Chaurasia, B., Goldau, J., Vogt, M.C., Ruud, J., Nguyen, K.D., Theurich, S., Hausen, A.C., Schmitz, J., Bronneke, H.S., Estevez, E., Allen, T.L., Mesaros, A., Partridge, L., Febbraio, M.A., Chawla, A., Wunderlich, F.T., Bruning, J.C., 2014. Signaling by IL-6 promotes alternative activation of macrophages to limit endotoxemia and obesity-associated resistance to insulin. *Nat Immunol* 15, 423-430.

Maynard, C.L., Harrington, L.E., Janowski, K.M., Oliver, J.R., Zindl, C.L., Rudensky, A.Y., Weaver, C.T., 2007. Regulatory T cells expressing interleukin 10 develop from Foxp3+ and Foxp3- precursor cells in the absence of interleukin 10. *Nat Immunol* 8, 931-941.

Mellman, I., 2013. Dendritic cells: master regulators of the immune response. *Cancer Immunol Res* 1, 145-149.

Meyer, P.C., 1966. Metastatic carcinoma of the pleura. *Thorax* 21, 437-443.

Mittal, S.K., Roche, P.A., 2015. Suppression of antigen presentation by IL-10. *Curr Opin Immunol* 34, 22-27.

Mocellin, S., Marincola, F., Rossi, C.R., Nitti, D., Lise, M., 2004. The multifaceted relationship between IL-10 and adaptive immunity: putting together the pieces of a puzzle. *Cytokine Growth Factor Rev* 15, 61-76.

Moore, K.W., de Waal Malefyt, R., Coffman, R.L., O'Garra, A., 2001. Interleukin-10 and the interleukin-10 receptor. *Annu Rev Immunol* 19, 683-765.

Moschos, C., Psallidas, I., Kollintza, A., Karabela, S., Papapetropoulos, A., Papiris, S., Light, R.W., Roussos, C., Stathopoulos, G.T., Kalomenidis, I., 2009. The angiopoietin/Tie2 axis mediates malignant pleural effusion formation. *Neoplasia* 11, 298-304.

Mosser, D.M., Edwards, J.P., 2008. Exploring the full spectrum of macrophage activation. *Nat Rev Immunol* 8, 958-969.

Muduly, D., Deo, S., Subi, T., Kallianpur, A., Shukla, N., 2011. An update in the management of malignant pleural effusion. *Indian J Palliat Care* 17, 98-103.

Mumm, J.B., Emmerich, J., Zhang, X., Chan, I., Wu, L., Mauze, S., Blaisdell, S., Basham, B., Dai, J., Grein, J., Sheppard, C., Hong, K., Cutler, C., Turner, S.,

LaFace, D., Kleinschek, M., Judo, M., Ayanoglu, G., Langowski, J., Gu, D., Paporello, B., Murphy, E., Sriram, V., Naravula, S., Desai, B., Medicherla, S., Seghezzi, W., McClanahan, T., Cannon-Carlson, S., Beebe, A.M., Oft, M., 2011. IL-10 elicits IFN γ -dependent tumor immune surveillance. *Cancer Cell* 20, 781-796.

Murthy, P., Ekeke, C.N., Russell, K.L., Butler, S.C., Wang, Y., Luketich, J.D., Soloff, A.C., Dhupar, R., Lotze, M.T., 2019. Making cold malignant pleural effusions hot: driving novel immunotherapies. *Oncoimmunology* 8, e1554969.

Naso, M.F., Liang, B., Huang, C.C., Song, X.Y., Shahied-Arruda, L., Belkowski, S.M., D'Andrea, M.R., Polkovitch, D.A., Lawrence, D.R., Griswold, D.E., Sweet, R.W., Amegadzie, B.Y., 2007. Dermokine: an extensively differentially spliced gene expressed in epithelial cells. *J Invest Dermatol* 127, 1622-1631.

Nasreen, N., Mohammed, K.A., Brown, S., Su, Y., Sriram, P.S., Moudgil, B., Loddenkemper, R., Antony, V.B., 2007. Talc mediates angiostasis in malignant pleural effusions via endostatin induction. *Eur Respir J* 29, 761-769.

O'Farrell, A.M., Liu, Y., Moore, K.W., Mui, A.L., 1998. IL-10 inhibits macrophage activation and proliferation by distinct signaling mechanisms: evidence for Stat3-dependent and -independent pathways. *EMBO J* 17, 1006-1018.

O'Garra, A., Barrat, F.J., Castro, A.G., Vicari, A., Hawrylowicz, C., 2008. Strategies for use of IL-10 or its antagonists in human disease. *Immunol Rev* 223, 114-131.

Ouyang, W., O'Garra, A., 2019. IL-10 Family Cytokines IL-10 and IL-22: from Basic Science to Clinical Translation. *Immunity* 50, 871-891.

Owen, J.L., Mohamadzadeh, M., 2013. Macrophages and chemokines as mediators of angiogenesis. *Front Physiol* 4, 159.

Park, J.S., Kim, Y.S., Jee, Y.K., Myong, N.H., Lee, K.Y., 2003. Interleukin-8 production in tuberculous pleurisy: role of mesothelial cells stimulated by cytokine network involving tumour necrosis factor- α and interleukin-1 β . *Scand J Immunol* 57, 463-469.

Peng, F., Xu, Z., Wang, J., Chen, Y., Li, Q., Zuo, Y., Chen, J., Hu, X., Zhou, Q., Wang, Y., Ma, H., Bao, Y., Chen, M., 2012. Recombinant human endostatin normalizes tumor vasculature and enhances radiation response in xenografted human nasopharyngeal carcinoma models. *PLoS One* 7, e34646.

Penny, H.L., Sieow, J.L., Adriani, G., Yeap, W.H., See Chi Ee, P., San Luis, B., Lee, B., Lee, T., Mak, S.Y., Ho, Y.S., Lam, K.P., Ong, C.K., Huang, R.Y.,

Ginhoux, F., Rotzschke, O., Kamm, R.D., Wong, S.C., 2016. Warburg metabolism in tumor-conditioned macrophages promotes metastasis in human pancreatic ductal adenocarcinoma. *Oncoimmunology* 5, e1191731.

Poczobutt, J.M., De, S., Yadav, V.K., Nguyen, T.T., Li, H., Sippel, T.R., Weiser-Evans, M.C., Nemenoff, R.A., 2016. Expression Profiling of Macrophages Reveals Multiple Populations with Distinct Biological Roles in an Immunocompetent Orthotopic Model of Lung Cancer. *J Immunol* 196, 2847-2859.

Poon, I.K., Lucas, C.D., Rossi, A.G., Ravichandran, K.S., 2014. Apoptotic cell clearance: basic biology and therapeutic potential. *Nat Rev Immunol* 14, 166-180.

Psallidas, I., Kalomenidis, I., Porcel, J.M., Robinson, B.W., Stathopoulos, G.T., 2016. Malignant pleural effusion: from bench to bedside. *Eur Respir Rev* 25, 189-198.

Psallidas, I., Kanellakis, N.I., Gerry, S., Thezenas, M.L., Charles, P.D., Samsonova, A., Schiller, H.B., Fischer, R., Asciak, R., Hallifax, R.J., Mercer, R., Dobson, M., Dong, T., Pavord, I.D., Collins, G.S., Kessler, B.M., Pass, H.I., Maskell, N., Stathopoulos, G.T., Rahman, N.M., 2018. Development and validation of response markers to predict survival and pleurodesis success in patients with malignant pleural effusion (PROMISE): a multicohort analysis. *Lancet Oncol* 19, 930-939.

Psallidas, I., Stathopoulos, G.T., Maniatis, N.A., Magkouta, S., Moschos, C., Karabela, S.P., Kollintza, A., Simoes, D.C., Kardara, M., Vassiliou, S., Papiris, S.A., Roussos, C., Kalomenidis, I., 2013. Secreted phosphoprotein-1 directly provokes vascular leakage to foster malignant pleural effusion. *Oncogene* 32, 528-535.

Redford, P.S., Murray, P.J., O'Garra, A., 2011. The role of IL-10 in immune regulation during *M. tuberculosis* infection. *Mucosal Immunol* 4, 261-270.

Rettew, A.N., Young, E.D., Lev, D.C., Kleinerman, E.S., Abdul-Karim, F.W., Getty, P.J., Greenfield, E.M., 2012. Multiple receptor tyrosine kinases promote the in vitro phenotype of metastatic human osteosarcoma cell lines. *Oncogenesis* 1, e34.

Rojiani, M.V., Ghoshal-Gupta, S., Kutiyawalla, A., Mathur, S., Rojiani, A.M., 2015. TIMP-1 overexpression in lung carcinoma enhances tumor kinetics and angiogenesis in brain metastasis. *J Neuropathol Exp Neurol* 74, 293-304.

Rose, S., Misharin, A., Perlman, H., 2012. A novel Ly6C/Ly6G-based strategy to analyze the mouse splenic myeloid compartment. *Cytometry A* 81, 343-350.

Rothlin, C.V., Carrera-Silva, E.A., Bosurgi, L., Ghosh, S., 2015. TAM receptor signaling in immune homeostasis. *Annu Rev Immunol* 33, 355-391.

Sabat, R., Grutz, G., Warszawska, K., Kirsch, S., Witte, E., Wolk, K., Geginat, J., 2010. Biology of interleukin-10. *Cytokine Growth Factor Rev* 21, 331-344.

Sahn, S.A., 1997. Pleural diseases related to metastatic malignancies. *Eur Respir J* 10, 1907-1913.

Saraiva, M., O'Garra, A., 2010. The regulation of IL-10 production by immune cells. *Nat Rev Immunol* 10, 170-181.

Satija, R., Farrell, J.A., Gennert, D., Schier, A.F., Regev, A., 2015. Spatial reconstruction of single-cell gene expression data. *Nat Biotechnol* 33, 495-502.

Sato, T., McCue, P., Masuoka, K., Salwen, S., Lattime, E.C., Mastrangelo, M.J., Berd, D., 1996. Interleukin 10 production by human melanoma. *Clin Cancer Res* 2, 1383-1390.

Savill, J.S., Henson, P.M., Haslett, C., 1989. Phagocytosis of aged human neutrophils by macrophages is mediated by a novel "charge-sensitive" recognition mechanism. *J Clin Invest* 84, 1518-1527.

Sharma, S., Stolina, M., Lin, Y., Gardner, B., Miller, P.W., Kronenberg, M., Dubinett, S.M., 1999. T cell-derived IL-10 promotes lung cancer growth by suppressing both T cell and APC function. *J Immunol* 163, 5020-5028.

Shouval, D.S., Ouahed, J., Biswas, A., Goettel, J.A., Horwitz, B.H., Klein, C., Muise, A.M., Snapper, S.B., 2014. Interleukin 10 receptor signaling: master regulator of intestinal mucosal homeostasis in mice and humans. *Adv Immunol* 122, 177-210.

Sikora, J.J., Dworacki, G.T., Kaczmarek, M.T., Jenek, R.E., Zeromski, J.O., 2004. Immunosuppressive mechanisms in the microenvironment of malignant pleural effusions. *Cancer Detect Prev* 28, 325-330.

Siveen, K.S., Sikka, S., Surana, R., Dai, X., Zhang, J., Kumar, A.P., Tan, B.K., Sethi, G., Bishayee, A., 2014. Targeting the STAT3 signaling pathway in cancer: role of synthetic and natural inhibitors. *Biochim Biophys Acta* 1845, 136-154.

Smith, N.L., Bromley, M.J., Denning, D.W., Simpson, A., Bowyer, P., 2015. Elevated levels of the neutrophil chemoattractant pro-platelet basic protein in macrophages from individuals with chronic and allergic aspergillosis. *J Infect Dis* 211, 651-660.

Soo, R.A., Chen, Z., Yan Teng, R.S., Tan, H.L., Iacopetta, B., Tai, B.C., Soong, R., 2018. Prognostic significance of immune cells in non-small cell lung cancer: meta-analysis. *Oncotarget* 9, 24801-24820.

Stathopoulos, G.T., Kalomenidis, I., 2012. Malignant pleural effusion: tumor-host interactions unleashed. *Am J Respir Crit Care Med* 186, 487-492.

Stathopoulos, G.T., Kollintza, A., Moschos, C., Psallidas, I., Sherrill, T.P., Pitsinos, E.N., Vassiliou, S., Karatza, M., Papiris, S.A., Graf, D., Orphanidou, D., Light, R.W., Roussos, C., Blackwell, T.S., Kalomenidis, I., 2007. Tumor necrosis factor-alpha promotes malignant pleural effusion. *Cancer Res* 67, 9825-9834.

Stathopoulos, G.T., Moschos, C., Loutrari, H., Kollintza, A., Psallidas, I., Karabela, S., Magkouta, S., Zhou, Z., Papiris, S.A., Roussos, C., Kalomenidis, I., 2008a. Zoledronic acid is effective against experimental malignant pleural effusion. *Am J Respir Crit Care Med* 178, 50-59.

Stathopoulos, G.T., Psallidas, I., Moustaki, A., Moschos, C., Kollintza, A., Karabela, S., Porfyridis, I., Vassiliou, S., Karatza, M., Zhou, Z., Joo, M., Blackwell, T.S., Roussos, C., Graf, D., Kalomenidis, I., 2008b. A central role for tumor-derived monocyte chemoattractant protein-1 in malignant pleural effusion. *J Natl Cancer Inst* 100, 1464-1476.

Stathopoulos, G.T., Sherrill, T.P., Karabela, S.P., Goleniewska, K., Kalomenidis, I., Roussos, C., Fingleton, B., Yull, F.E., Peebles, R.S., Jr., Blackwell, T.S., 2010. Host-derived interleukin-5 promotes adenocarcinoma-induced malignant pleural effusion. *Am J Respir Crit Care Med* 182, 1273-1281.

Stathopoulos, G.T., Zhu, Z., Everhart, M.B., Kalomenidis, I., Lawson, W.E., Bilaceroglu, S., Peterson, T.E., Mitchell, D., Yull, F.E., Light, R.W., Blackwell, T.S., 2006. Nuclear factor-kappaB affects tumor progression in a mouse model of malignant pleural effusion. *Am J Respir Cell Mol Biol* 34, 142-150.

Steinbrink, K., Jonuleit, H., Muller, G., Schuler, G., Knop, J., Enk, A.H., 1999. Interleukin-10-treated human dendritic cells induce a melanoma-antigen-specific anergy in CD8(+) T cells resulting in a failure to lyse tumor cells. *Blood* 93, 1634-1642.

Stitt, T.N., Conn, G., Gore, M., Lai, C., Bruno, J., Radziejewski, C., Mattsson, K., Fisher, J., Gies, D.R., Jones, P.F., et al., 1995. The anticoagulation factor protein S and its relative, Gas6, are ligands for the Tyro 3/Axl family of receptor tyrosine kinases. *Cell* 80, 661-670.

Sturlan, S., Oberhuber, G., Beinhauer, B.G., Tichy, B., Kappel, S., Wang, J., Rogy, M.A., 2001. Interleukin-10-deficient mice and inflammatory bowel disease associated cancer development. *Carcinogenesis* 22, 665-671.

Sun, B., Zhang, Y., 2014. Overview of orchestration of CD4+ T cell subsets in immune responses. *Adv Exp Med Biol* 841, 1-13.

Tanikawa, T., Wilke, C.M., Kryczek, I., Chen, G.Y., Kao, J., Nunez, G., Zou, W., 2012. Interleukin-10 ablation promotes tumor development, growth, and metastasis. *Cancer Res* 72, 420-429.

Villena Garrido, V., Cases Viedma, E., Fernandez Villar, A., de Pablo Gafas, A., Perez Rodriguez, E., Porcel Perez, J.M., Rodriguez Panadero, F., Ruiz Martinez, C., Salvatierra Velazquez, A., Valdes Cuadrado, L., 2014. Recommendations of diagnosis and treatment of pleural effusion. Update. *Arch Bronconeumol* 50, 235-249.

Voll, R.E., Herrmann, M., Roth, E.A., Stach, C., Kalden, J.R., Girkontaite, I., 1997. Immunosuppressive effects of apoptotic cells. *Nature* 390, 350-351.

Waldmann, T.A., 2018. Cytokines in Cancer Immunotherapy. *Cold Spring Harb Perspect Biol* 10.

Wan, Y.Y., Flavell, R.A., 2005. Identifying Foxp3-expressing suppressor T cells with a bicistronic reporter. *Proc Natl Acad Sci U S A* 102, 5126-5131.

Wang, F., Yang, L., Gao, Q., Huang, L., Wang, L., Wang, J., Wang, S., Zhang, B., Zhang, Y., 2015. CD163+CD14+ macrophages, a potential immune biomarker for malignant pleural effusion. *Cancer Immunol Immunother* 64, 965-976.

Wang, T., Ge, Y., Xiao, M., Lopez-Coral, A., Azuma, R., Somasundaram, R., Zhang, G., Wei, Z., Xu, X., Rauscher, F.J., 3rd, Herlyn, M., Kaufman, R.E., 2012. Melanoma-derived conditioned media efficiently induce the differentiation of monocytes to macrophages that display a highly invasive gene signature. *Pigment Cell Melanoma Res* 25, 493-505.

Weber-Nordt, R.M., Meraz, M.A., Schreiber, R.D., 1994. Lipopolysaccharide-dependent induction of IL-10 receptor expression on murine fibroblasts. *J Immunol* 153, 3734-3744.

Wu, X.Z., Zhai, K., Yi, F.S., Wang, Z., Wang, W., Wang, Y., Pei, X.B., Shi, X.Y., Xu, L.L., Shi, H.Z., 2019. IL-10 promotes malignant pleural effusion in mice by regulating TH 1- and TH 17-cell differentiation and migration. *Eur J Immunol*.

Yang, L., Wang, F., Wang, L., Huang, L., Wang, J., Zhang, B., Zhang, Y., 2015. CD163+ tumor-associated macrophage is a prognostic biomarker and is associated with therapeutic effect on malignant pleural effusion of lung cancer patients. *Oncotarget* 6, 10592-10603.

Yano, S., Herbst, R.S., Shinohara, H., Knighton, B., Bucana, C.D., Killion, J.J., Wood, J., Fidler, I.J., 2000a. Treatment for malignant pleural effusion of human lung adenocarcinoma by inhibition of vascular endothelial growth factor receptor tyrosine kinase phosphorylation. *Clin Cancer Res* 6, 957-965.

Yano, S., Shinohara, H., Herbst, R.S., Kuniyasu, H., Bucana, C.D., Ellis, L.M., Fidler, I.J., 2000b. Production of experimental malignant pleural effusions is dependent on invasion of the pleura and expression of vascular endothelial growth factor/vascular permeability factor by human lung cancer cells. *Am J Pathol* 157, 1893-1903.

Ye, Z.J., Zhou, Q., Gu, Y.Y., Qin, S.M., Ma, W.L., Xin, J.B., Tao, X.N., Shi, H.Z., 2010. Generation and differentiation of IL-17-producing CD4+ T cells in malignant pleural effusion. *J Immunol* 185, 6348-6354.

Ye, Z.J., Zhou, Q., Yin, W., Yuan, M.L., Yang, W.B., Xiang, F., Zhang, J.C., Xin, J.B., Xiong, X.Z., Shi, H.Z., 2012a. Interleukin 22-producing CD4+ T cells in malignant pleural effusion. *Cancer Lett* 326, 23-32.

Ye, Z.J., Zhou, Q., Yin, W., Yuan, M.L., Yang, W.B., Xiong, X.Z., Zhang, J.C., Shi, H.Z., 2012b. Differentiation and immune regulation of IL-9-producing CD4+ T cells in malignant pleural effusion. *Am J Respir Crit Care Med* 186, 1168-1179.

Yeh, H.H., Lai, W.W., Chen, H.H., Liu, H.S., Su, W.C., 2006. Autocrine IL-6-induced Stat3 activation contributes to the pathogenesis of lung adenocarcinoma and malignant pleural effusion. *Oncogene* 25, 4300-4309.

Yuetiva Deming, F.F., Francesca Cignarella, Claudia Cantoni, Simon Hsu, Robert Mikesell, Zeran Li, Jorge L Del-Aguila, Umber Dube, Fabiana Geraldo Farias, Joseph Bradley, Bruno Benitez, John Budde, Laura Ibanez, Maria Victoria Fernandez, 2018. The MS4A gene cluster is a key regulator of soluble TREM2 and Alzheimer disease risk. *bioRxiv*.

Zagorska, A., Traves, P.G., Lew, E.D., Dransfield, I., Lemke, G., 2014. Diversification of TAM receptor tyrosine kinase function. *Nat Immunol* 15, 920-928.

Zamboni, M.M., da Silva, C.T., Jr., Baretta, R., Cunha, E.T., Cardoso, G.P., 2015. Important prognostic factors for survival in patients with malignant pleural effusion. *BMC Pulm Med* 15, 29.

Zebrowski, B.K., Yano, S., Liu, W., Shaheen, R.M., Hicklin, D.J., Putnam, J.B., Jr., Ellis, L.M., 1999. Vascular endothelial growth factor levels and induction of permeability in malignant pleural effusions. *Clin Cancer Res* 5, 3364-3368.

Zeni, E., Mazzetti, L., Miotto, D., Lo Cascio, N., Maestrelli, P., Querzoli, P., Pedriali, M., De Rosa, E., Fabbri, L.M., Mapp, C.E., Boschetto, P., 2007. Macrophage expression of interleukin-10 is a prognostic factor in nonsmall cell lung cancer. *Eur Respir J* 30, 627-632.

Zheng, G.X., Terry, J.M., Belgrader, P., Ryvkin, P., Bent, Z.W., Wilson, R., Ziraldo, S.B., Wheeler, T.D., McDermott, G.P., Zhu, J., Gregory, M.T., Shuga, J., Montesclaros, L., Underwood, J.G., Masquelier, D.A., Nishimura, S.Y., Schnall-Levin, M., Wyatt, P.W., Hindson, C.M., Bharadwaj, R., Wong, A., Ness, K.D., Beppu, L.W., Deeg, H.J., McFarland, C., Loeb, K.R., Valente, W.J., Ericson, N.G., Stevens, E.A., Radich, J.P., Mikkelsen, T.S., Hindson, B.J., Bielas, J.H., 2017. Massively parallel digital transcriptional profiling of single cells. *Nat Commun* 8, 14049.

Zhong, H., Han, B.H., Dong, Q.G., Feng, J.X., Bao, G.L., Sha, H.F., Su, J.Z., 2004. [Efficient generation and functional characteristics of dendritic cells from malignant pleural effusion in patients with lung cancer]. *Zhonghua Jie He He Hu Xi Za Zhi* 27, 542-545.

Zhu, J., Yamane, H., Paul, W.E., 2010. Differentiation of effector CD4 T cell populations (*). *Annu Rev Immunol* 28, 445-489.

Zlotnik, A., Yoshie, O., 2012. The chemokine superfamily revisited. *Immunity* 36, 705-716.

7. List of abbreviations

ACRE	apoptotic cell response element
APC	antigen-presenting cell
ARG1	arginase 1
BPE	benign pleural effusion
CCL	C-C motif chemokine ligand
CCR	C-C motif chemokine receptor
CSIF	the cytokine synthesis inhibitory factor
CTL	cytotoxic T lymphocytes
CXCL	C-X-C motif chemokine ligand
DC	dendritic cell
ECM	extracellular matrix
FDR	false discovery rate
GAS6	growth-arrest-specific 6
GO	gene ontology
Gpx1	glutathione peroxidase-1
Hmox1	heme oxygenase-1
IL	interleukin
LLC	Lewis lung carcinoma
LPS	lipopolysaccharide
MAPK	mitogen-activated protein kinase
MDSC	myeloid-derived suppressor cell
MHC	major histocompatibility
MMP	metalloproteinase
MPE	malignant pleural effusion
NSCLC	non-small cell lung cancer
Pbx-1b	pre-B-cell leukemia transcription factor-1b
PDL1	programmed cell death 1 ligand 1
PROS1	protein S
PRR	pattern recognition receptor
PtdSer	phosphatidylserine
RTK	receptor tyrosine kinase
SEMA4D	semaphorin 4D
STAT3	signal transducers and activators of transcription 3
TGFβ	transforming growth factor
TIMP1	tissue inhibitor of metalloproteinases 1
TLR	Toll-like receptors
TNF	tumor necrosis factor
Treg	regulatory T cell

Trem2	encoding triggering receptor expressed on myeloid cells 2
UMI	unique molecular identifier
PFS	progression free survival
PPE	parapneumonic pleural effusion
VEGF	vascular endothelial growth factor
visNE	visualization of t-distributed stochastic neighbor embedding
scRNA-seq	single cell RNA sequencing
SPF	specific-pathogen-free
SPP1	secreted phosphoprotein-1
TAM	Tyro3-Axl-Mertk
Th cells	T helper cells
TrPE	transudative pleural effusion
t-SNE	t-stochastic neighbor embedding

8. Acknowledgement

The PhD's life is about to end in the blink of an eye. Looking back over these three years, I have not only gained a lot of knowledge, but I have also matured a lot. I am grateful to the supervisors and colleagues for teaching me knowledge over the past three years. I am also grateful for all the experiences during this time for my training, so that I can confidently and firmly face future work and life.

I would like to thank the entire Department of General Visceral and Thoracic Surgery, University Medical Center Hamburg-Eppendorf (UKE) for the support which enlightened me in making this PhD thesis a success.

In particular, I wish to acknowledge the support and wisdom received from my PhD supervisor, Professor Nicola Gagliani. Professor Gagliani is knowledgeable and has great academic achievements. From designing the project, processing the experiments, the creating the first draft, to the revision and improvement, the requirements of Professor Gagliani for my thesis have been very strict, Professor Gagliani has also given very serious and careful guidance. I admire this professor for his rigorous and pragmatic research spirit. In the words of a Chinese saying: "listening the words of a wise man can be superior to studying ten years of books."

I would like to acknowledge and thank Dr. Anastasios Giannou, Mustafa Shiri and the amazing colleagues at the UKE. Thank you for helping me to conduct this study and for embracing the work of this research so wholeheartedly.

I would like to acknowledge the China Scholarship Council for funding my stay in Germany. I am truly grateful for the support they provided and without it this study would not have been possible.

Last but not least, thank you to my parents and my wife for their endless love and encouragement.

9. Curriculum Vitae

Personal Information

Name: Zhao, Lilan

Date of Birth: 10/10/1991

Gender: Male

Nationality: Chinese

Email: zhaolilan1991@gmail.com

Telephone: 0176 3013 5689

Educational Background

Oct, 2016: Start of MD study at University Medical Center Hamburg-Eppendorf, Hamburg, Germany

Sep, 2014-Jul, 2016: Master of Clinical Medicine, Tongji University, Shanghai, PR of China

Sep, 2009-Jul, 2014: Bachelor of Clinical Medicine, Tongji University, Shanghai, PR of China

Awards and Honors

1. Scholarship from China Scholarship Council; China Scholarship Council (2016).
2. Scholarship of Academic Excellence (2009-2015)
3. Graduate student reward fund for international academic conferences (2015)
4. Tongji University "Excellence Cup" Award (2015)
5. Student Innovation Training Program VIII Award (2013)
6. Student Innovation Training Program VI Award (2011)

Academic Experience

Sep 2014-Jun 2016. Residency Training in Shanghai Pulmonary Hospital, Tongji University, Shanghai, P.R.China

September 6-9, 2015. Oral presentation: Visceral pleural invasion in non-small cell lung cancer. A SEER database analysis. The 16th World Conference on Lung Cancer (WCLC). Denver, Colorado, USA.

Jun 2013- Jun 2014. Internship in Shanghai Tongji Hospital, Tongji University, Shanghai, P.R.China.

10. Eidesstattliche Versicherung

Ich versichere ausdrücklich, dass ich die Arbeit selbständig und ohne fremde Hilfe verfasst, andere als die von mir angegebenen Quellen und Hilfsmittel nicht benutzt und die aus den benutzten Werken wörtlich oder inhaltlich entnommenen Stellen einzeln nach Ausgabe (Auflage und Jahr des Erscheinens), Band und Seite des benutzten Werkes kenntlich gemacht habe.

Ferner versichere ich, dass ich die Dissertation bisher nicht einem Fachvertreter an einer anderen Hochschule zur Überprüfung vorgelegt oder mich anderweitig um Zulassung zur Promotion beworben habe.

Ich erkläre mich einverstanden, dass meine Dissertation vom Dekanat der Medizinischen Fakultät mit einer gängigen Software zur Erkennung von Plagiaten überprüft werden kann.

Unterschrift: